JOHANNES KEPLER
UNIVERSITÄT LINZ | JKU

TNF

Technisch-Naturwissenschaftliche
Fakultät

Homotopy Methods for Nonlinear Magnetostatics

MASTERARBEIT

zur Erlangung des akademischen Grades

Diplomingenieur

im Masterstudium

Industriemathematik

Eingereicht von:
Stefan Mühlböck

Angefertigt am:
Institut für Numerische Mathematik

Beurteilung:
A. Univ.-Prof. Dipl.-Ing. Dr. Walter Zulehner

Linz, Mai, 2010

Abstract

Starting point is a nonlinear system of equations. One possibility to solve this problem is Newton's method, which is only locally convergent. In order to obtain an appropriate starting value for Newton's method we want to consider so-called homotopy methods. Thereby a crucial point is to find a continuous transition from an easily solvable problem to the original nonlinear problem by introducing a so-called homotopy parameter. In other words a known (or easily computable) solution is connected with the exact solution by a continuous function which we want to follow numerically. Therefore we present several strategies for following such curves.

Another main part of this thesis is how to control the step size of such a method in order to derive an efficient and robust method to follow the solution curve. The step length adaptation strategy is based on asymptotic expansion.

The simulation of electromagnetic phenomena – e.g. in magnetic valves or electric motors – requires a fast solution of large scaled nonlinear system of equations, arising from the Finite-Element-discretized underlying partial differential equation (PDE). This thesis is concerned with a two-dimensional magnetostatic field problem. Starting from Maxwell's equations, the mathematical model is derived, which is the variational formulation of a boundary value problem. An important feature of magnetic field problems is the nonlinear relation between the fields $\mathbf{B}$ and $\mathbf{H}$. The corresponding B-H-curve must in general be approximated from measurements. In this thesis we use an analytic function as B-H-curve.
Existence of a unique solution for the continuous problem is shown under natural (physical) assumptions.

Finally, numerical results verify the efficiency of the homotopy methods, tested on an one-dimensional model problem of an electric motor.

Another application of this one-dimensional problem is obtained by using a natural parameter instead of the homotopy parameter. The area of the coils is enlarged in every step. With this parameter we try to simulate the rotation of the motor. With the obtained numerical results we see how the solution is related to the natural parameter in this rotation problem.

Zusammenfassung

Ausgangpunkt ist ein System von nichtlinearen Gleichungen. Eine Möglichkeit dieses zu lösen, besteht durch das bekannte Newton-Verfahren, welches jedoch nur lokal konvergent ist. Um einen geeigneten Startwert für das Newton-Verfahren zu bekommen, betrachten wir sogenannte Homotopie-Verfahren. Ein essentieller Punkt dabei ist, eine stetige Verbindung von einem einfach lösbaren Problem zum originalen nichtlinearen Problem zu finden, indem man einen sogenannten Homotopie-Parameter einführt. Anders ausgedrückt wird eine bekannte (oder leicht berechenbare) Lösung mit der exakten Lösung durch eine stetige Funktion verbunden, welcher wir numerisch folgen wollen. Wir präsentieren einige unterschiedliche Strategien, um solchen Kurven zu folgen.

Ein weiterer Schwerpunkt dieser Arbeit ist wie man die Schrittweite solcher Verfahren kontrolliert steuern kann, um eine möglichst effiziente und stabile Methode für die Kurvenverfolgung zu produzieren. Diese Schrittweitensteuerung basiert auf asymptotischer Entwicklung.

Die Simulation elektromagnetischer Vorgänge – z. B. in Magnetventilen oder Elektromotoren – verlangt eine effiziente Lösung von großdimensionalen nichtlinearen Gleichungssystemen, welche aus der Finite-Elemente-Diskretisierung der zugrundeliegenden partiellen Differentialgleichungen (PDE) entstehen. Die vorliegende Masterarbeit behandelt ein zweidimensionales magnetostatisches Feldproblem. Zunächst wird ausgehend von den Maxwell'schen Gleichungen das mathematische Modell hergeleitet. Eine wichtige Rolle spielt der nichtlineare Zusammenhang zwischen **B**- und **H**-Feld. Die dazugehörige B-H-Kurve muss in der Regel aus Messwerten approximiert werden. In dieser Arbeit verwenden wir eine analytische Funktion als B-H-Kurve.
Existenz einer eindeutigen Lösung des kontinuierlichen Problems wird unter natürlichen (physikalischen) Voraussetzungen gezeigt.

Schließlich bestätigen numerische Resultate die Effizienz des Verfahrens anhand eines eindimensionalen Testbeispiels eines Elektromotors.

Eine weitere Anwendung dieses eindimensionalen Problems wird erhalten, indem man anstatt des Homotopie-Parameters einen natürlichen Parameter verwendet. Der Bereich der Spulen wird nun in jedem Schritt vergrößert. Mit diesem Parameter versuchen wir nun die Rotation des Motors zu simulieren. Anhand der erhaltenen numerischen Resultate sehen wir, wie sich die Lösung mit dem natürlichen Parameter in diesem Rotationsproblem ändert.

Acknowledgement

First of all, I would like to express my thanks to my supervisor Prof. Walter Zulehner, for giving me the chance to write this thesis. I am also grateful for inspiring discussions and vital hints during the development of this thesis and the associated implementations.

Furthermore, I am indebted to Markus Kollmann for constructive remarks, his patience in answering all the questions that arose, and his valuable time. Moreover I thank Mykhaylo Yudytskiy for various discussions and help in programming and debugging attempts.

I would not be able to reach this stage of my life without the help and support of my family. I am deeply grateful to my parents, Annaliese and Anton, for their belief in me.

Last but not least I acknowledge the Institute of Computational Mathematics at the Johannes Kepler University of Linz for the technical support.

Stefan Mühlböck
Linz, May 2010

Contents

1 Introduction **1**

2 The Basic Concept of Homotopy Methods **5**
2.1 General Problem Description 5
2.2 The Homotopy Method 6

3 Implicitly Defined Curves **12**

4 Numerical Path Following **16**
4.1 Staircase method 16
4.2 Euler's method 18
4.3 Predictor - Corrector method 19
4.4 Pseudo - Arc Length Approximation 20

5 Step Size Control **24**
5.1 Step Length Adaptation by Asymptotic Expansion 24
5.2 Interpretation of the Quantities κ and δ 27
5.2.1 The Contraction Rate κ 27
5.2.2 The Distance to the Curve δ 29

6 Numerical Path Following for Parameter Dependent Problems **31**

7 Derivation of the Physical Problem **33**
7.1 Physical Model 33
7.1.1 Maxwell's equations 33
7.1.2 Material laws 36
7.2 Mathematical Model 37
7.2.1 Reduction to 2D 37
7.2.2 Variational Formulation 39
7.2.3 Existence and Uniqueness of the Solution 41

8 A 1D Model Problem and its Discretization **42**
8.1 Finite Element Method for the Boundary Value Problem . . . 43
8.2 The geometry of the motor 46
8.3 B-H-Curve Approximation 47

9 A Parameter Dependent Problem **49**

10 Numerical Results **56**
10.1 Homotopy Methods 56
10.2 Numerical Results for a Parameter Dependent Problem 58

11 Conclusion and Future Work **62**

Bibliography **64**

Eidesstattliche Erklärung **67**

Curriculum Vitae **68**

List of Figures

2.1 The curve $x(t)$ 8

3.1 Different possibilities for the curve $x(t)$ 12
3.2 A function $x(t)$ with turning points 14

4.1 A staircase method for following $x(t)$ 17
4.2 Euler's method for following $x(t)$ 19
4.3 A predictor-corrector method for following $x(t)$ 20
4.4 A pseudo-arc length approximation 21

5.1 One predictor-corrector step 29
5.2 A $\widetilde{\delta}$-tube around $u(t)$ 29
5.3 Interpretation of $\widetilde{\delta}$ 30

7.1 Cross section of the model motor 34

8.1 One-dimensional model of a motor 46
8.2 B-H-Curve from real-life measurements 48
8.3 $f^{-1}(s)$ 48

9.1 Rotation of the motor: Starting position and first rotation step 50
9.2 Rotation of the motor: k-th and l-th rotation step 51
9.3 One-dimensional model of a motor with fixed interfaces 51
9.4 Start-configuration 52
9.5 End-configuration 52

10.1 Numerical results: PC-method without step length control . . 59

List of Tables

10.1 Numerical results: Homotopy I and Homotopy II 58
10.2 Numerical results: Parameter Dependent Problem with start-step size $\sigma = 1/5$ 60
10.3 Numerical results: Parameter Dependent Problem with start-step size $\sigma = 1/8$ 60
10.4 Numerical results: Parameter Dependent Problem with start-step size $\sigma = 1/10$ 61

Chapter 1

Introduction

This thesis deals with the solution of nonlinear magnetostatic field problems by so-called homotopy methods. A strong focus is put on the nonlinearity. The whole thesis is mainly based on the book from Eugene L. Hallower and Kurt Georg [8].

The topic was motivated by a cooperation with the ACCM (Austrian Center of Competence in Mechatronics) and is based on results obtained in the project seminar in computational mathematics held in the summer semester 2008 at Johannes Kepler University Linz (cf. Bachelor thesis from A. Lechner and S. Mühlböck [12]). The main task of this seminar was to advance the process of optimization of the degree of efficiency by shape optimization. One way was discussed by Elisabeth Frank and Markus Kollmann, namely shape optimization by shape derivatives (cf. [5] and [9]).

In the magnetostatic case, under certain symmetry assumptions, the system of partial differential equations (PDEs) initially in 3D can be reduced to a single PDE in two dimensions. Its solution directly determines the magnetic field and the magnetic induction, whose fields are usually of interest. This static two-dimensional model is used in many applications, at least to extract partial information about the magnetic behavior of the underlying problem.

The nonlinearity occurs in a material relation between the magnetic field $\mathbf{H}$ and the magnetic induction $\mathbf{B}$. The relation can be expressed by the so-called B-H-curve, or the closely related reluctivity ν.

With suitable boundary conditions, the magnetostatic 2D-problem can be formulated in a nonlinear variational formulation.
In [12] a damped Newton method is used to compute the solution of a one-

dimensional model problem. There it was easy to see that the method wastes a lot of computational time - in several problem specifications more than 30 iterations are needed to compute a sufficiently accurate approximation of the exact solution.

It is known that Newton's method is only locally convergent. One motivation of this thesis now is to use another method to solve this one-dimensional model problem with as few iterations as possible- in any case, less than 30 iterations. One possibility to produce an appropriate starting point for Newton's method is a homotopy method, or continuation method as it is also called. Thereby we produce a globally convergent method to solve our problem.

Another motivation of this thesis is a so-called parameter dependent problem and the application of numerical continuation methods for such a problem. Thereby it is not important to follow the curve as fast as possible. In this context it is sometimes essential to traverse the curve very closely in order to get precise information about the considered quantities.

In the solution of the nonlinear variational formulation three quintessential components are involved:

1. The **Finite Element Method (FEM)** is used to discretize the continuous, infinite dimensional problem. For an introduction we recommend [10] and [14].
2. The **homotopy method** is used to produce an appropriate starting point for Newton's method. It is an important task to find a good starting value in order to take advantage of the local quadratic convergence, instead of damping which results in slow linear convergence.
3. **Newton's method** tackles the nonlinearity. In each step of Newton's iterations a linear system of equations has to be solved.

The tasks of this thesis:
In this thesis we want to get an idea of the behavior of a homotopy method for solving a one-dimensional problem. This happens in the following way:

- Introduce the concept of homotopy methods.
- Apply these methods to a derived one-dimensional model of an electric motor.
- Compare the results and draw conclusions.

The organization of this thesis:

- Chapter 2: The Basic Concept of Homotopy Methods

  The main problem under consideration is presented. A short introduction into homotopy methods, along with the motivation for why such methods are needed is given. Then, the properties of a homotopy method are briefly discussed. Also different examples for homotopy maps are mentioned. Finally the so-called global homotopy is introduced.

- Chapter 3: Implicitly Defined Curves

  First we introduce the concept of regular points and regular values. The assumptions under which a continuous connection between the starting problem and the original problem exists are discussed. Moreover curves with occurring turning points are considered.

- Chapter 4: Numerical Path Following

  Several different methods for following the continuous curve from the initial point to the exact solution of the original problem are discussed and compared. Finally the principle of predictor-corrector methods is introduced.

- Chapter 5: Step Size Control

  A strategy to produce an efficient and robust predictor-corrector method with a step size controlling procedure based on asymptotic expansion is presented. The discussion is closely related to one step length adaptation in [8]. Finally a short interpretation of the used quantities is presented.

- Chapter 6: Numerical Path Following for Parameter Dependent Problems

  The concept of parameter dependent problems is presented. Finally the application of numerical path following methods for such problems is discussed.

- Chapter 7: Derivation of the Physical Problem

  Starting from the physical model for magnetostatics, i.e. Maxwell's equations, the mathematical formulation is derived, namely the boundary value problem for a nonlinear partial differential equation. One part is the discussion of the solvability of this PDE. At the same time, conditions on the nonlinear parameter are derived.

- Chapter 8: A 1D Model Problem and its Discretization

  For discretization we introduce an one-dimensional problem. After a short introduction on the Finite Element Method (cf. [12, 14]), FEM is applied to the variational formulation of the problem. The discussion of the approximation of the B-H-curve (cf. [11, 12]) is also a part of this chapter.

- Chapter 9: A Parameter Dependent Problem

  We use a natural parameter to set up parameter dependent problem. The stepwise rotation of the two-dimensional model of the electric motor is discussed. For simplicity the rotation is simulated by the 1D-model for the motor by changing the area of the coils in every rotation step.

- Chapter 10: Numerical Results

  The theoretical results are used in numerical studies, tested on a 1D-model for an electric motor. The results obtained by homotopy methods are presented. Also numerical results for a parameter dependent problem are discussed.

- Chapter 11: Conclusion and Future Work

  The results are summarized and conclusions about possible continuations are drawn.

Chapter 2

The Basic Concept of Homotopy Methods

This chapter is mainly based on [8] and [15]. First we discuss the motivation of so-called homotopy methods in our context. Some advantages of this method compared with the classical Newton's method are mentioned. Then the whole idea and the principle of such methods is introduced. Finally, the way to choose a so-called homotopy mapping is discussed by several examples.

2.1 General Problem Description

Let us consider the following problem setting (cf. [13]):
We want to find a solution to a system of n nonlinear equations in n variables, say

$$F(x) = 0, \tag{2.1}$$

where $F : \mathbb{R}^n \to \mathbb{R}^n$ and $x = (x_1, x_2, \ldots, x_n)^T$. Equation (2.1) can be written componentwise in the form

$$\begin{aligned} F_1(x_1, x_2, \ldots, x_n) &= 0, \\ F_2(x_1, x_2, \ldots, x_n) &= 0, \\ &\vdots \\ F_n(x_1, x_2, \ldots, x_n) &= 0, \end{aligned}$$

where $F_i : \mathbb{R}^n \to \mathbb{R}$ for $i = 1, 2, \ldots, n$. Since there exists in general no direct methods for solving such nonlinear equations (2.1), iterative methods are used to obtain a solution of (2.1).
The most famous method for finding successively better approximations to

the roots of nonlinear equations is Newton's method. Thereby each iteration consists of three steps:

1. Compute $F(x^{(k)})$ and $F'(x^{(k)})$.
2. Solve the linear system $F'(x^{(k)})s^{(k)} = -F(x^{(k)})$.
3. Set $x^{(k+1)} = x^{(k)} + s^{(k)}$.

Here, $F'(x)$ is the Jacobian of F at the point x, which is given by

$$F'(x) = \begin{pmatrix} \frac{\partial F_1}{\partial x_1}(x) & \frac{\partial F_1}{\partial x_2}(x) & \cdots & \frac{\partial F_1}{\partial x_n}(x) \\ \frac{\partial F_2}{\partial x_1}(x) & \frac{\partial F_2}{\partial x_2}(x) & \cdots & \frac{\partial F_2}{\partial x_n}(x) \\ \vdots & \vdots & \ddots & \vdots \\ \frac{\partial F_n}{\partial x_1}(x) & \frac{\partial F_n}{\partial x_2}(x) & \cdots & \frac{\partial F_n}{\partial x_n}(x) \end{pmatrix}.$$

The big advantage of Newton's method is its fast convergence. Under appropriate requirements it converges quadratically. Possible disadvantages are:

- The computational costs: If n is large the computation of $F'(x)$ as well as solving the linear system can be very costly.
- The method converges locally. A good initial guess must be known.

In the following we will reduce or eliminate these disadvantages. One possibility are so-called homotopy methods.

2.2 The Homotopy Method

Starting point of the derivation is the following initial value problem:

$$\begin{aligned} x'(s) &= -F'(x(s))^{-1}F(x(s)) \\ x(0) &= x_0 \end{aligned} \tag{2.2}$$

Now we are able to introduce the idea of a Newton path.

Definition 2.1 (Newton path)**.**
A solution $z : [0, \infty) \to \mathbb{R}^n$ of the initial value problem (2.2) with

$$\lim_{s\to\infty} z(s) = x^* \text{ and } F(x^*) = 0.$$

is called a Newton path.

From now on let $z(s)$ be a Newton path. Applying chain rule to the identity

$$y(s) \;=\; F(z(s)),$$

we obtain

$$\begin{aligned} y'(s) &= F'(z(s))z'(s) = -F'(z(s))F'(z(s))^{-1}F(z(s)) \\ &= -F(z(s)) = -y(s). \end{aligned}$$

Using the initial conditions

$$x(0) = z(0) = x^0,$$

it follows that

$$y(0) = F(z(0)) = F(x^0),$$

and

$$y(s) \;=\; e^{-s}F(x^0).$$

So for all $s \in [0, \infty)$

$$F(z(s)) \;=\; e^{-s}F(x^0).$$

By $\phi : [0, 1] \to [0, \infty]$, $s = \phi(t)$ with

$$e^{-s} \;=\; 1 - t$$

a different parametrization of the Newton path is defined. For

$$x(t) \;=\; z(\phi(t)),$$

it follows that

$$F(x(t)) \;=\; (1 - t)F(x^0)$$

for $t \in [0, 1]$. So, $x(t)$ is a solution of the equation

$$H(x, t) \;=\; 0 \tag{2.3}$$

with

$$H(x,t) \quad = \quad F(x(t)) - (1-t)F(x^0) \tag{2.4}$$

for all $t \in [0,1]$.

Under appropriate assumptions on the nonlinear mapping F, the existence of a solution $x(t)$ of (2.3) for all $t \in [0,1]$ is guaranteed. A more comprehensive theoretical background can be found in [15].

The function $x : [0,1] \to \mathbb{R}^n$ connects the given initial value $x^0 = x(0)$ continuously with the solution $x^* = x(1)$, e.g. in Figure 2.1.

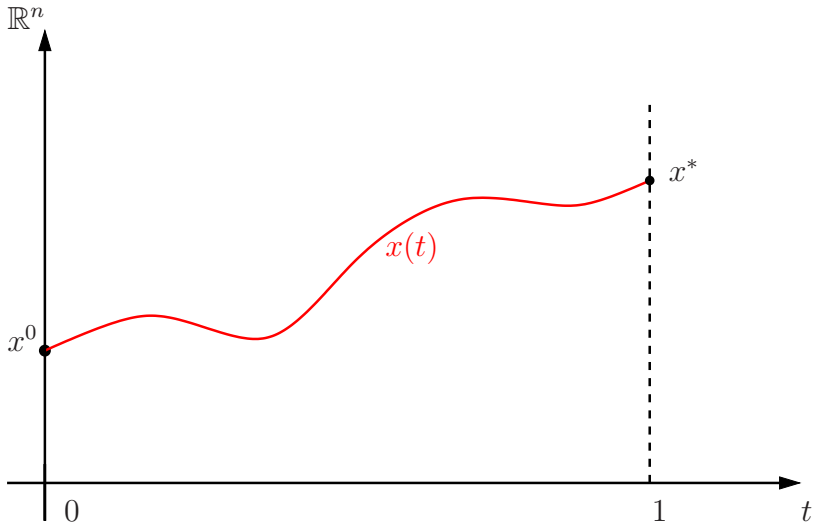

Figure 2.1: The curve $x(t)$

This leads to the following strategy for computing the solution x^* of the original problem (2.1):

Starting from the known value x^0 at $t = 0$, one follows (numerically) the graph of the function $x : [0,1] \to \mathbb{R}^n, t \in [0,1]$, until the solution x^* is reached at $t = 1$.
This strategy is not restricted to the mapping (2.3). More generally, the original equation

$$F(x) \quad = \quad 0$$

has to be embedded into a family of equations

$$H(x,t) \quad = \quad 0 \tag{2.5}$$

by introducing a parameter $t \in [0,1]$.

The mapping $H : \mathbb{R}^n \times [0,1] \to \mathbb{R}^n$ has to fulfill the following properties:

1. The starting problem (for $t = 0$)

$$H(x,0) \quad = \quad 0$$

   has a known (or easily computable) solution x^0, i.e. $H(x^0, 0) = 0$.

2. The equation (for $t = 1$)

$$H(x,1) \quad = \quad 0$$

   is equivalent to the original equation (2.1), i.e. $H(x,1) = F(x)$.

Thereby

- H is called a homotopy map (or embedding),
- t is called homotopy parameter and
- the equation (2.5) is called a homotopy equation.

We consider again the identity

$$H(x,t) \quad = \quad F(x) - (1-t)F(x^0) \tag{2.6}$$

for $t \in [0,1]$.

Now we discuss the required properties of the homotopy map H. We obtain for

- $t = 0$: $H(x,0) = F(x) - F(x^0) \Rightarrow x = x^0$ is a solution, and for
- $t = 1$: $H(x,1) = F(x) = 0 \Rightarrow$ original problem.

It is reasonable to assume that H is continuous in t, i.e. a continuous transition from an easily solvable problem to the original problem is given by the mapping H.

Remark 2.2. To set up a continuous problem which transforms the problem is easy. The hard part is that the solution should also depend continuously on t.

In the following part we want to consider some examples for admissible homotopy mappings (cf. [7],[8],[15]):

Example 2.3. A frequently used homotopy is the so-called convex homotopy

$$H(x,t) \;=\; tF(x) + (1-t)G(x),$$

where $G : \mathbb{R}^n \to \mathbb{R}^n$ is a given mapping with a known point x^0 such that $G(x^0) = 0$. H connects the starting problem

$$G(x) \;=\; 0$$

continuously with the original equation

$$F(x) \;=\; 0.$$

Example 2.4. Another possibility is the global homotopy, discussed above. Thereby we only have to replace $G(x)$ in the previous example by

$$G(x) = F(x) - F(x^0).$$

Then we obtain

$$H(x,t) = tF(x) + (1-t)\Big(F(x) - F(x^0)\Big) = F(x) - (1-t)F(x^0).$$

We have already discussed the properties of this homotopy map.

Example 2.5. A different choice is given by

$$G(x) = x - x^0.$$

Then the homotopy map reads

$$H(x,t) = tF(x) + (1-t)(x - x^0).$$

Since for $t = 0$:

$$H(x, 0) = x - x^0 = 0$$

and for $t = 1$:

$$H(x, 1) = F(x) = 0$$

the required properties on the homotopy map are fulfilled.

In the remaining chapters we use the global homotopy

$$H(x, t) \quad = \quad F(x) - (1 - t)F(x^0).$$

The hope is that the continuous change of the equations also leads to a continuous change of the solutions to (2.3). Then it would be possible to follow the curve of solutions numerically, as it was described before. Such a strategy is called a homotopy method (also: embedding method, continuation method).
In the following chapter we study the question whether there exists a curve of solutions (homotopy path) for general homotopies.

Chapter 3

Implicitly Defined Curves

This chapter is mainly based on the discussion in [15]. First we introduce the concept of regular points and regular values. Using these definitions, the assumptions under which a continuous connection between the starting problem and the original problem exists are discussed. Finally the whole concept is considered for curves with occurring turning points.

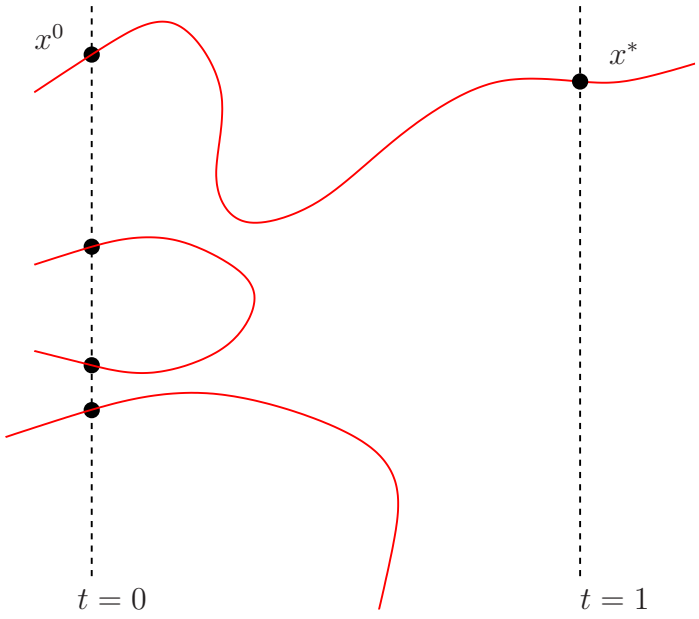

Figure 3.1: Different possibilities for the curve $x(t)$

We realize that several questions immediately arise:

1. When is it assured that a curve $x(t)$ exists and is smooth?

2. If such a curve exists, when is it assured that it will intersect the target homotopy level $t = 1$ in a finite length?

3. How can we numerically trace such a curve?

To answer the last question we refer to Chapter 4. The first and the second question are answered by the implicit function theorem. Therefore the following definition is of central importance.

Definition 3.1. Let $p, q \in \mathbb{N}$ with $p \geq q$ and let $f : \mathbb{R}^p \to \mathbb{R}^q$ be a continuously differentiable function.

1. A point $x \in \mathbb{R}^p$ is called a regular point of f if $f'(x)$ has rank q.

2. A value $y \in \mathbb{R}^q$ is called a regular value of f if all $x \in \mathbb{R}^p$ with $f(x) = y$ are regular points of f.

In the case $p = q$, 0 is a regular value of f if and only if all solutions of $f(x) = 0$ are simple. If 0 is a regular value of $H(\cdot, 0)$, then the implicit function theorem guarantees the existence of a curve of solutions $x(t)$ in a neighborhood of $t = 0$. From this the following theorem (see [15]) can be derived:

Theorem 3.2. *Let $H : \mathbb{R}^n \times \mathbb{R} \to \mathbb{R}^n$ be a continuously differentiable mapping and let $x^0 \in \mathbb{R}^n$ be a point with $H(x^0, 0) = 0$. If 0 is a regular value of $H(\cdot, t)$ for all $t \in \mathbb{R}$, then we have for the connected component $\mathcal{C}(x^0, 0) \subset \mathbb{R}^n \times \mathbb{R}$ of $H^{-1}(0)$ which contains $(x^0, 0)$:*
There is a continuously differentiable function $x : (a, b) \to \mathbb{R}^n$,
$a, b \in \mathbb{R} \cup \{\pm\infty\}, a < b$ with

$$\mathcal{C}(x^0, 0) \quad = \quad \{(x(t), t) : t \in (a, b)\}$$

and $\|x(t)\| \to \infty$ for $t \to a$ if $a > -\infty$ and for $t \to b$ if $b < +\infty$.

Proof. The proof is based on the implicit function theorem and can be found in [15].

□

So $\mathcal{C}(x^0, 0)$ is the image of a continuously differentiable curve, which can be parameterized by t. Then the known solution x^0 can still be connected with the solution x^* by a continuous curve.

However, t is not necessarily monotonically increasing along $\mathcal{C}(x^0, 0)$. There might exist so-called turning points where the monotonicity with respect to t changes (e.g. in Figure 3.2).

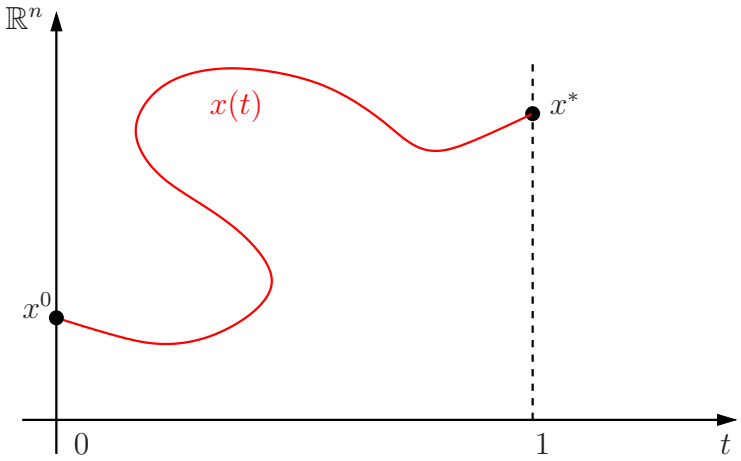

Figure 3.2: A function $x(t)$ with turning points

For the following discussion of the more general situation, it is advantageous to combine the vector $x \in \mathbb{R}^n$ and the homotopy parameter $t \in \mathbb{R}$ into a single vector u of $n+1$ unknowns, such that

$$u \quad = \quad (x, t) \in \mathbb{R}^{n+1}.$$

The homotopy equation (2.3) then becomes an under-determined system of equations

$$H(u) \quad = \quad 0 \tag{3.1}$$

with $H : \mathbb{R}^{n+1} \to \mathbb{R}^n$ of n equations for $n+1$ unknowns. The curve u is now parameterized in a different way, e.g. a parametrization with respect to the arclength. The known solution of the starting problem and the solution of the original equation correspond to special points in $\mathbb{R}^{n+1}$:

$$u^0 = (x^0, 0) \quad \text{and} \quad u^* = (x^*, 1).$$

These two points are special solutions of $H(u) = 0$ and

- u^0 lies on the hyperplane $\mathbb{R}^n \times \{0\}$.
- u^* lies on the hyperplane $\mathbb{R}^n \times \{1\}$.

Therefore we have the following generalization of Theorem 3.2:

Theorem 3.3. *Assume that $H : \mathbb{R}^{n+1} \to \mathbb{R}^n$ is a continuously differentiable mapping and let $u^0 \in \mathbb{R}^{n+1}$ be a point with $H(u^0) = 0$. If 0 is a regular value of H, then we have for the connected component $\mathcal{C}(u^0) \subset \mathbb{R}^{n+1}$ of $H^{-1}(0)$ which contains u^0:*
There is a continuously differentiable function $u : \mathbb{R} \to \mathbb{R}^{n+1}$ with $u(0) = u^0, u'(s) \neq 0$ for all $s \in \mathbb{R}$ and

$$\mathcal{C}(u^0) \quad = \quad u(\mathbb{R})$$

and either u is injective and $\|u(s)\| \to \infty$ for $s \to \pm\infty$ or u is periodic.

Proof. See [15].

□

We can now state the main result of this chapter.

Remark 3.4. If zero is a regular value of H, then the solution curve u is defined on the whole $\mathbb{R}$ and either the curve is diffeomorphic to a circle or the curve is diffeomorphic to the real line.
So the solution curve which connects the solution of the original problem u^0 with the exact solution of the original problem u^* is given by $H^{-1}(0)$.

In the following chapter we try to follow such curves in order to obtain the exact solution.

Chapter 4

Numerical Path Following

From the previous discussion we know under which conditions a curve, which connects the solution of the starting problem u^0 with the solution of the original problem u^*, exists. Our task now is to follow this solution curve with as few steps as possible. Therefore we present some different strategies to achieve this (cf. [8, 15]).

In this method we first subdivide the interval $[0, 1]$ in not necessarily equidistant subintervals by introducing $t_0, \ldots, t_m$ such that

$$0 = t_0 < t_1 < \cdots < t_m = 1.$$

In other words the t-axis is divided into subintervals.

The first method that we consider arises from the most natural possibility to follow a solution curve. It is called the staircase method.

4.1 Staircase method

We start at $t_0 = 0$. From the requirements on the initial point we already know that $x(t_0) = x^0$. So the first point on the solution curve is (x^0, t_0).
By choosing a step size $\Delta t_0 > 0$ we obtain the next point t_1 by

$$t_1 = t_0 + \Delta t_0.$$

Because of the continuity of $x(t)$ the point $x(t_0)$ is close to $x(t_1)$ for small step sizes Δt_0. So, we can expect that Newton's method for the equation

$$H(x, t_1) \;=\; 0$$

with starting value x^0 converges to the exact solution $x^1 = x(t_1)$. In this way, a new point (x^1, t_1) on our solution curve is obtained.

For the next step we choose a new step size $\Delta t_1 > 0$. So the next point on the t-axis is given by

$$t_2 = t_1 + \Delta t_1.$$

By the similar statement as above we can expect that Newton's method for the equation

$$H(x, t_2) \quad = \quad 0$$

with starting value x^1 converges to the exact solution $x^2 = x(t_2)$, such that the next point on the solution curve is (x^2, t_2).

This strategy can be repeated until we finally reach a solution x^* of the original problem (2.1) at $t_m = 1$.

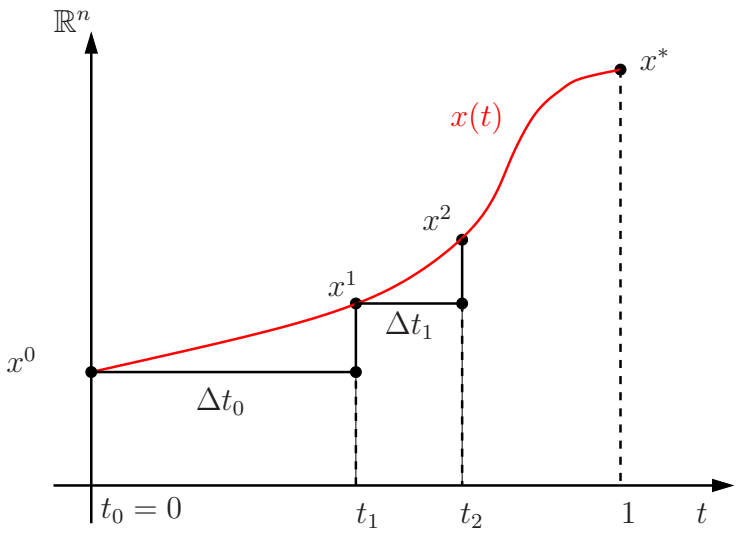

Figure 4.1: A staircase method for following $x(t)$

The next method is the so-called Euler's method. For some convergence results of this method we refer to [16].

4.2 Euler's method

For this method we need some preliminary work. By differentiating the identity

$$H(x(t),t) \;=\; 0$$

one obtains by using the chain rule

$$\frac{\partial H}{\partial x}(x(t),t)x'(t) + \frac{\partial H}{\partial t}(x(t),t) \;=\; 0,$$

the so-called Davidenko differential equation. If $\frac{\partial H}{\partial x}(x(t),t)$ is nonsingular, the differential equation can also be written in the explicit form

$$x'(t) \;=\; \underbrace{-\Big(\frac{\partial H}{\partial x}(x(t),t)\Big)^{-1}\frac{\partial H}{\partial t}(x(t),t)}_{:=g(x(t),t)}.$$

The solution curve $x(t)$ solves this differential equation. So, we can also use methods for initial value problems in order to follow numerically the solution curve. Therefore we use Euler's method.

We again start at $t_0 = 0$ and choose a step size $\Delta t_0 > 0$, such that again

$$t_1 = t_0 + \Delta t_0.$$

Then Euler's method produces the following approximation of the solution at the point t_1:

$$\begin{aligned} x(t_1) \;&\approx\; x(t_0) + \Delta t_0 x'(t_0) \\ &=\; x^0 + \Delta t_0 g(x^0, t_0) =: \widetilde{x}^1 \end{aligned}$$

In the next step we again choose a new step size $\Delta t_1 > 0$. So, again, one obtains an approximation to $x(t_2)$ by Euler's method, which is given by

$$x(t_2) \;\approx\; \widetilde{x}^1 + \Delta t_1 g(\widetilde{x}^1, t_1) =: \widetilde{x}^2,$$

where

$$t_2 = t_1 + \Delta t_1.$$

This strategy can be repeated until we reach an approximation $\widetilde{x}^*$ to the exact solution x^* of the original problem (2.1) at $t_m = 1$ (see Figure 4.2).

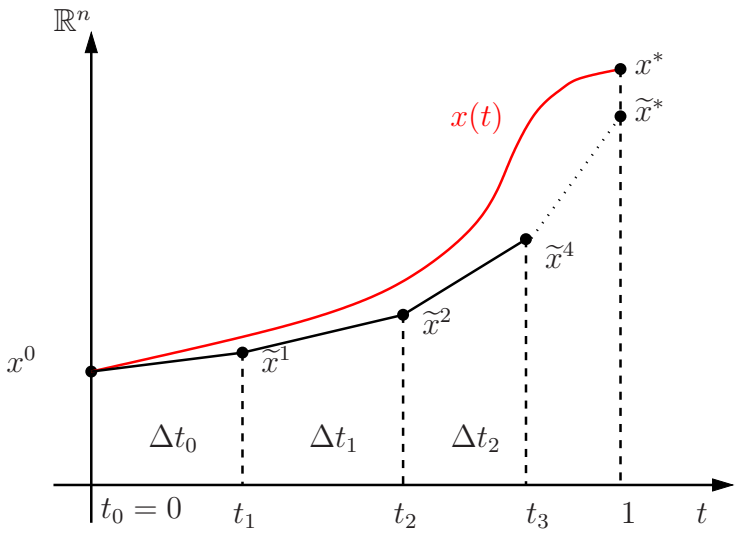

Figure 4.2: Euler's method for following $x(t)$

4.3 Predictor - Corrector method

So far we know two different methods to follow the solution curve. Another approach is to combine this two strategies into a single method consisting of three substeps:

1. Choose a step size $\Delta t_0 > 0$.
2. Predictor step: Use Euler's method to compute
$$\widetilde{x}^1 \quad := \quad x^0 + \Delta t_0 g(x^0, t_0).$$
3. Corrector step: Solve
$$H(x, t_1) \quad = \quad 0$$
by Newton's method with starting value $\widetilde{x}^1$.

With this strategy we obtain a new point on the solution curve. We can repeat these three steps until we reach a solution x^* of the original problem (2.1) at $t_m = 1$ (Figure 4.3). Such a method is called a predictor-corrector method, or a PC-method for short.

One can easily see that a PC-method is an improvement compared with both methods - the staircase method and Euler's method. If we match the staircase method with a predictor-corrector method one can easily see, that after

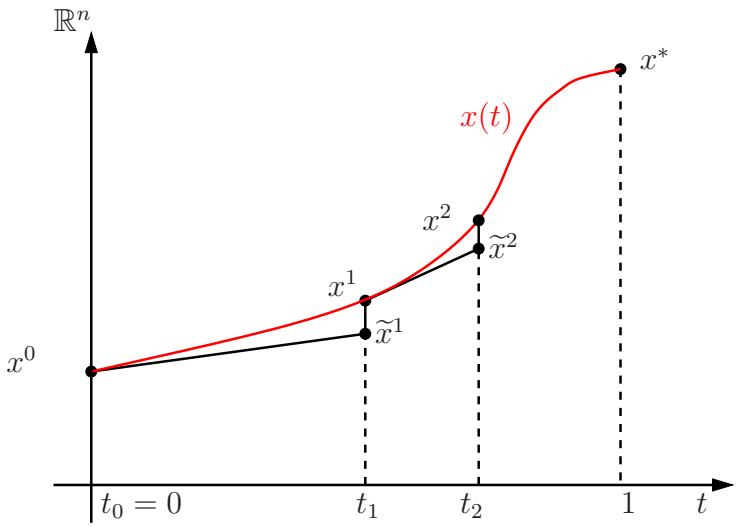

Figure 4.3: A predictor-corrector method for following $x(t)$

performing one step, we have a better initial value for the next step in a PC-method than in the staircase method. Moreover a PC-method guarantees, that we traverse the solution curve very close to the curve, what is not guaranteed by Euler's method.

4.4 Pseudo - Arc Length Approximation

All methods discussed so far are not able to deal with turning points like in Figure 3.2. Such curves are not parameterizable by the homotopy parameter t, but we can do a so-called pseudo-arc length approximation. In this context the following definition is of central importance:

Definition 4.1. Let A be a $n \times (n+1)$-matrix with $rank(A) = n$. The unique vector $v = v(A) \in \mathbb{R}^{n+1}$ satisfying the three conditions

1. $Av = 0$;
2. $\|v\| = 1$;
3. $\det \begin{pmatrix} A \\ v^T \end{pmatrix} > 0$;

is called the tangent vector induced by A.

The first condition fixes the direction, the second fixes the length and the last one fixes the sign of the tangent vector. If we set $A = H'(u^0)$ we get the direction tangent to the solution at $u^0 = (x^0, 0)$. In order to guarantee that the curve is traced always in the same direction, the sign of the determinant is not allowed to change. Now we are able to traverse a solution curve with occurring turning points.

Our initial point is again u^0. For a given step size $\Delta s_0 > 0$ the predictor step is given by

$$\widetilde{u}^1 \quad = \quad u^0 + \Delta s_0 v^0,$$

where $v^0 = v(A)$ with $A = H'(u^0)$, or in other words v^0 is the tangent vector induced by $H'(u^0)$.

So far, the points produced in the corrector step all lie in the fixed hyperplane $\mathbb{R}^n \times \{t_1\}$. Now it is required that the iterates of the corrector step lie in that hyperplane which contains the point $\widetilde{u}^1$ and whose normal direction is the tangent direction v^0 (see Figure 4.4).Thus in this approach we consider a turned hyperplane.

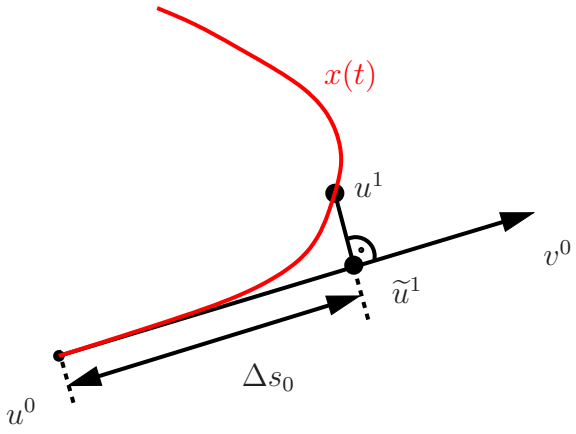

Figure 4.4: A pseudo-arc length approximation

This hyperplane is described by the equation

$$(v^0)^T(u^1 - \widetilde{u}^1) \quad = \quad 0. \tag{4.1}$$

Moreover, the iterates are required to lie on the solution curve, hence

$$H(u^1) \quad = \quad 0. \tag{4.2}$$

Now we solve the system (4.1), (4.2) by Newton's method with starting value $\widetilde{u}^1$. For performing the first step of Newton's method the following linear system has to be solved:

$$\begin{pmatrix} H'(\widetilde{u}^1) \\ (v^0)^T \end{pmatrix} \Delta u \;=\; -\begin{pmatrix} H(\widetilde{u}^1) \\ 0 \end{pmatrix}, \tag{4.3}$$

where

$$\Delta u \;=\; \widehat{u}^1 - \widetilde{u}^1$$

and $\widehat{u}^1$ is the first iterate of Newton's method. For the next step we use a similar technique with the new starting value $\widehat{u}^1$. We repeat this process until the next point u^1 on the solution curve u is reached.

Algorithm 4.1 sketches a particular version of the predictor-corrector method incorporating an Euler predictor step and the Newton's methods, described above, as a corrector.

```
1  input
2      begin
3          u^0 ∈ R^{n+1} such that H(u^0) = 0;        initial point
4          Δs_0 > 0;                                  initial step length
5      end
6
7  repeat
8      ũ^1 := u^0 + Δs_0 v^0;                         predictor step
9      repeat
10         compute Δu via (4.3);                      corrector loop
11         û^1 = ũ^1 + Δu;
12         ũ^1 = û^1;
13     until convergence;
14     u^0 = û^1;                                     new point along H^{-1}(0)
15     choose a new step length Δs_0 > 0;             step length adaptation
16 until the solution u* is reached.
```

Algorithm 4.1: A predictor-corrector method

An algorithm, similar to the one presented above is easily derivable for all other methods described in this chapter.

Remark 4.2. Observe that a practical implementation will usually not lead to points which lie exactly on the solution curve after the corrector step. One stops the corrector iteration at a sufficiently good approximation and continues with the next predictor step. For a homotopy method it is not desirable to spend a lot of computational work for computing intermediate points. It is more important to reach $t = 1$ at a good approximation to the exact solution as fast as possible. Therefore, the main focus in practical implementation is an efficient step size control and a good convergence indicator for the corrector step.

So far we did not consider how to choose the optimal step length in order to obtain an efficient homotopy method. In the next chapter we present such a strategy how to control the step size process. This step length adaptation is based on asymptotic expansion.

Chapter 5

Step Size Control

So far the step length was uniformly constant throughout. This is of course not efficient for any practical implementation. To some extent of course, the step length strategy depends upon the accuracy with which it is desired to trace a solution curve numerically. In any case, an efficient algorithm for this task needs to incorporate an automatic strategy for controlling the step length.

This chapter is mainly based on [8]. There we use step length adaptation by asymptotic expansion. Other possibilities (cf. [8]) are for example the step length adaptation of Den Heijer & Rheinboldt or the step length strategies involving variable order predictors.

5.1 Step Length Adaptation by Asymptotic Expansion

The basic idea in this approach is to observe the performance of the corrector procedure and then to adapt the step length $\sigma > 0$ accordingly. More precisely, suppose that a point $u \in H^{-1}(0)$ has been obtained. Suppose further that a step length $\sigma > 0$ is given. The predictor point is given by

$$\widetilde{u}(\sigma) = u + \sigma v$$

with $v = v(A)$ and $A = H'(u)$. Then an iterative corrector process is performed to generate a next point $z(\sigma) \in H^{-1}(0)$.

The step length strategies which we discuss in this section are based on a-posteriori estimates of the performance of the corrector process in order to answer the following question:

Given the manner in which the corrector process starting at $\widetilde{u}(\sigma)$ is performed, which step length $\widetilde{\sigma}$ would have been the "best" for obtaining $z(\widetilde{\sigma})$ from u?

This "ideal" step length $\widetilde{\sigma}$ is determined via asymptotic estimates, and it is then taken as the step length for the next predictor step. This strategy depends primarily upon two factors:

- The particular predictor-corrector method being utilized.
- The criteria used in deciding what performance is considered "best".

If u and $\widetilde{u}(\sigma)$ are given as we discussed above, we obtain the first corrector point $w(\sigma)$ from the solution of a linear system of equations which we solve in each iteration of Newton's method. If this solution is denoted by s, then $w(\sigma)$ is given by

$$w(\sigma) \quad = \quad \widetilde{u}(\sigma) + s.$$

Now we are able to define the following two important factors:

- The first corrector step length

  $$\delta(\widetilde{u}(\sigma), \sigma) \quad := \quad \|s\|, \tag{5.1}$$

  which approximates the distance to the curve.

- The quotient of the first two successive Newton steps

  $$\kappa(\widetilde{u}(\sigma), \sigma) \quad := \quad \frac{\delta(w(\sigma), \sigma)}{\delta(\widetilde{u}(\sigma), \sigma)}, \tag{5.2}$$

  which is called the contraction rate of the corrector process. Since Newton's method is locally quadratically convergent, it is clear that $\kappa(\widetilde{u}(\sigma), \sigma)$ will decrease (and hence Newton's method will become faster) if σ decreases and hence $\widetilde{u}(\sigma)$ approaches $H^{-1}(0)$.

The following lemma characterizes the asymptotic behavior of $\kappa(u, \sigma)$ with respect to σ.

Lemma 5.1. *Suppose that $x(t)$ has non-zero curvature at the point u, then*

$$\kappa(u, \sigma) \quad = \quad \kappa_2(u)\sigma^2 + \mathcal{O}(\sigma^3) \tag{5.3}$$

for some constant $\kappa_2(u) \geq 0$ which is independent of σ and depends smoothly on u.

Proof. The proof can be found in [8]. □

The following lemma characterizes the asymptotic behavior of $\delta(u,\sigma)$ with respect to σ.

Lemma 5.2. *The following asymptotic expansions hold:*

$$\delta(u,\sigma) \;=\; \delta_2(u)\sigma^2 + \mathcal{O}(\sigma^3), \tag{5.4}$$

where the asymptotic constant $\delta_2(u)$ is independent of σ and depends smoothly on u.

Proof. The proof is similar to the proof of Lemma 5.1. □

In the view of the asymptotic behavior of $\kappa(u,\sigma)$ in (5.3) the step length modification $\sigma \to \widetilde{\sigma}$ is now easy to explain. Assume that a predictor-corrector step has been performed with step length σ. Then $\delta(w(\sigma),\sigma)$ and $\delta(u,\sigma)$ will have been calculated and thus $\kappa(u,\sigma)$ can be obtained without any significant additional cost. Now we rewrite (5.3), such that

$$\kappa_2(u) \;=\; \frac{\kappa(u,\sigma)}{\sigma^2} + \mathcal{O}(\sigma). \tag{5.5}$$

In order to have a robust and efficient PC-method we want to adapt continually the step length σ so that a nominal prescribed contraction rate $\widetilde{\kappa}$ is maintained. The choice of $\widetilde{\kappa}$ will generally depend upon the nature of the problem at hand, and on the desired security with which we want to traverse the solution curve. That is, the smaller $\widetilde{\kappa}$ is chosen, the greater will be the security with which the PC-method will follow the curve.
Once $\widetilde{\kappa}$ has been chosen, we will consider a step length $\widetilde{\sigma}$ to be adequate if $\kappa(u,\widetilde{\sigma}) \approx \widetilde{\kappa}$. By using (5.2) and (5.5) and neglecting higher order terms we obtain the formula

$$\widetilde{\sigma} \;=\; \sigma\sqrt{\frac{\widetilde{\kappa}}{\kappa(u,\sigma)}} \tag{5.6}$$

as a step length for the next predictor step.

By fixing a nominal distance $\widetilde{\delta}$ we obtain a further step length adaptation by an analogous technique as above

$$\widetilde{\sigma} \;=\; \sigma\sqrt{\frac{\widetilde{\delta}}{\delta(u,\sigma)}}, \tag{5.7}$$

where $\delta(u,\sigma)$ is the distance which is measured after performing the current predictor-corrector step.

In order to formulate a safeguarded curve tracing algorithm, we recommend monitoring several factors such as those outlined above. Thus, at any point several adequate step lengths $\widetilde{\sigma}$ are calculated and the smallest of these possibilities is then chosen as the step length for the next predictor step.

Algorithm 5.1 sketches how the above described step length adaptations can be incorporated into a predictor-corrector method such as Algorithm 4.1.

The evaluation of $\delta(u,\sigma)$ and $\kappa(u,\sigma)$ is available at essentially no additional cost after performing the first and second steps respectively in the corrector loop. If the observed quantities $\kappa(u,\delta)$ or $\delta(u,\sigma)$ exceed a certain tolerance above the nominal values, the predictor step is repeated with a reduced step length. This test is performed within the corrector loop in order to avoid unnecessary corrector steps which would in any event be discarded later.

5.2 Interpretation of the Quantities κ and δ

So far we did not talk about how the quantities $\widetilde{\kappa}$ and $\widetilde{\delta}$ should be chosen. Therefore we want to illuminate the following two quantities:

5.2.1 The Contraction Rate κ

Assume that the last obtained point on the solution curve $u(t)$ is denoted by u^0. With a predictor step we achieve the point $\widetilde{u}^1$. In this subsection we use the notation $\widetilde{u}^1 = \widehat{u}^0$. We take this point as a starting point for the iterative corrector loop. This procedure generates a sequence of points $(\widehat{u}^j)_{j=1,\ldots,m}$, where $\widehat{u}^m$ is a sufficiently accurate approximation of u^1, which is the next point on the solution curve $u(t)$ (see Figure 5.1).

Let s^j denote the j-th corrector step for $j = 1, \ldots, m$ given by

$$s^j \;:=\; \widehat{u}^j - \widehat{u}^{j-1}.$$

input
  begin
    $u^0 \in \mathbb{R}^{n+1}$ such that $H(u^0) = 0$; initial point
    $\sigma > 0$; initial step length
    $\widetilde{\kappa}$; nominal contraction rate
    $\widetilde{\delta}$; nominal distance to curve
  end

repeat
  $\widetilde{u}^1 := u^0 + \sigma v^0$; predictor step
  repeat
    compute Δu via (4.3); corrector loop
    $\widehat{u}^1 = \widetilde{u}^1 + \Delta u$;
    calculate $\delta(\widetilde{u}^1, \sigma)$ and $\kappa(\widetilde{u}^1, \sigma)$; cf. (5.1), (5.2)
    if $\delta(\widetilde{u}^1, \sigma) > \widetilde{\delta}$ or $\kappa(\widetilde{u}^1, \sigma) > \widetilde{\kappa}$;
      repeat predictor step with PC-step not accepted
      reduced step size σ;
    $\widetilde{u}^1 = \widehat{u}^1$;
  until convergence;
  $f := \max\left\{\sqrt{\frac{\kappa(\widetilde{u}^1,\sigma)}{\widetilde{\kappa}}}, \sqrt{\frac{\delta(\widetilde{u}^1,\sigma)}{\widetilde{\delta}}}\right\}$; cf. (5.3), (5.4)
  $f := \max\left\{\min\left\{f, 2\right\}, \frac{1}{10}\right\}$; deceleration factor $f \in \left[\frac{1}{10}, 2\right]$
  $\sigma := \frac{\sigma}{f}$; step length adaptation using
    deceleration factor f
  $u^0 = \widehat{u}^1$; new point along $H^{-1}(0)$
  until the solution u^* is reached.

Algorithm 5.1: A predictor-corrector method with step length adaptations

Then the contraction rate is given by

$$\kappa(\widehat{u}^j, \sigma) \quad := \quad \frac{\|s^{j+1}\|}{\|s^j\|}.$$

We already discussed that the choice of $\widetilde{\kappa}$ will generally depend on the desired security with which we want to traverse the solution curve. That is, the smaller $\widetilde{\kappa}$ is chosen, the greater will be the security with which the predictor-corrector method will follow the curve.

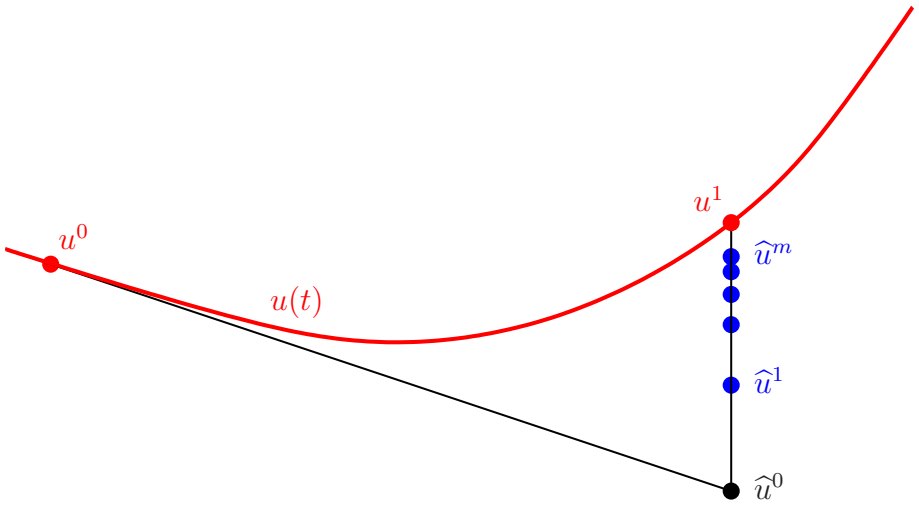

Figure 5.1: One predictor-corrector step

5.2.2 The Distance to the Curve δ

We already discussed that δ approximates the distance to the curve. So if we choose the nominal distance to the curve $\widetilde{\delta}$ we fix a tube along the solution curve $u(t)$ (see Figure 5.2).

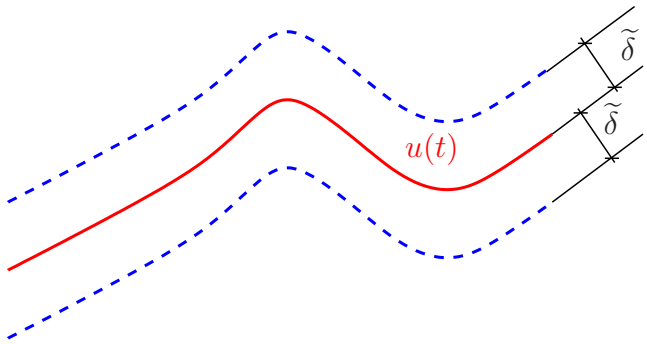

Figure 5.2: A $\widetilde{\delta}$-tube around $u(t)$

With this technique we can guarantee that the solution curve is always traversed in a fixed distance to the curve. If the step size σ is too large we run out of this security distance. So we have to choose a smaller step size σ_{new} and repeat the predictor step with σ_{new} (see Figure 5.3).

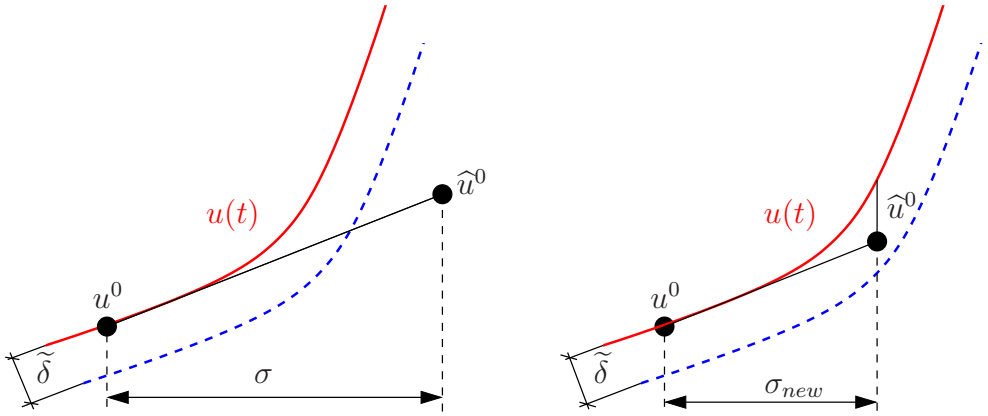

Figure 5.3: A predictor step with too large step length σ (left) and with new step length σ_{new}(right)

Remark 5.3. In order to obtain an efficient step length controlling procedure the hard job is to find an optimal setting for the nominal quantities $\widetilde{\kappa}$ and $\widetilde{\delta}$. This setting depends on how accurate we want the computed intermediate results to be. On the one hand if $\widetilde{\delta}$ is large, we go very fast forward to the exact solution, but we need many corrector steps to come back to the solution curve. On the other hand if $\widetilde{\kappa}$ is small we have very accurate intermediate results, but therefore also many corrector steps are required. So for choosing these two quantities in first line it is very important to save the computational costs.
Many examples how to choose $\widetilde{\kappa}$ and $\widetilde{\delta}$ can be found in the chapter of numerical results (see Chapter 10).

Chapter 6

Numerical Path Following for Parameter Dependent Problems

So far we have introduced an artificial homotopy parameter $t \in [0, 1]$. Thereby, the equation

$$F(x) \;=\; 0$$

has to be embedded into a family of equations

$$H(x, t) \;=\; 0.$$

For the choice of the homotopy map H there exist several different possibilities, e.g. the global homotopy

$$H(x, t) \;=\; F(x) - (1 - t)F(x^0).$$

For such kind of numerical continuation methods it is important to compute the solution of the problem with as few iterations as possible.

But there also exist other problems, where the parameter is naturally involved. Typical sources of such problems are discretizations of boundary value problems involving such a natural parameter. From now on, we will call such problems parameter dependent problems.

The problem under consideration has now the form

$$H(u, t) \;=\; 0,$$

where t denotes the natural parameter. Without loss of generality we can assume that the parameter t belongs to $[0, 1]$.

The main goal of methods for parameter dependent problems is to gain information about the behavior of the solution u in dependence of the natural parameter t. We want to traverse the solution curve by a numerical path following method, as was discussed in the previous chapter. In this context it is sometimes essential to follow the curve very closely to obtain a sufficiently accurate result.

Thus, in addition to the homotopy methods to obtain an appropriate starting value for Newton's method we have a second motivation to use numerical path following methods.

In Chapter 9 we will consider a parameter dependent problem, in which we will simulate the behavior of an electric motor by turning the rotor at small angles. To follow the solution curve numerically we use a predictor-corrector method as we discussed it in Chapter 4.

Chapter 7

Derivation of the Physical Problem

In the previous chapters we derived details to homotopy methods. Thus far, we are able to solve nonlinear problems with the help of such methods. Such nonlinear problems are for example magnetostatic problems. We now try to solve such problems with the above discussed homotopy methods. First of all we have to derive a mathematical model of the problem. This derivation is mainly based on [6], [11] and [12].

Starting point of our discussion was a model problem of an electric motor sketched in Figure 7.1, which was provided by the group of the ACCM (Austrian Center of Competence in Mechatronics). The area A7 is the permanent magnet of the motor. Areas A1 up to A6 are the coils. Between the coils and the permanent magnet there is a little air gap. Area A8 is an iron layer.

7.1 Physical Model

7.1.1 Maxwell's equations

Maxwell's equations are used to describe electromagnetic phenomena:

$$curl\ \mathbf{H} = \mathbf{J} + \frac{\partial \mathbf{D}}{\partial t}, \tag{7.1}$$

$$curl\ \mathbf{E} = -\frac{\partial \mathbf{B}}{\partial t}, \tag{7.2}$$

$$div\ \mathbf{B} = 0, \tag{7.3}$$

$$div\ \mathbf{D} = \rho. \tag{7.4}$$

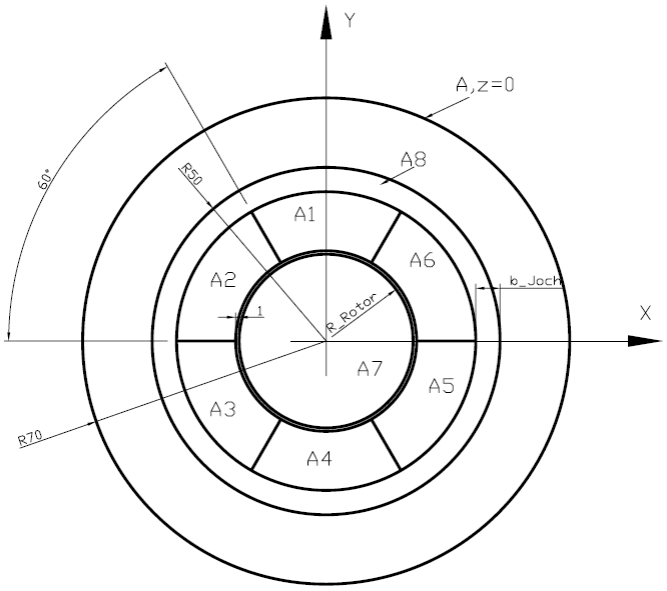

Figure 7.1: Motor

The quantities involved are

H	-	magnetic field,
E	-	electric field,
B	-	magnetic flux,
D	-	electric induction,
J	-	electric current density,
ρ	-	electric charge density.

All these quantities depend on the position in space $x = (x_1, x_2, x_3)$ and on the time t. The boldface letters are vector fields.
Via constitutive laws there exists a relation between the magnetic flux **B** and the magnetic field **H**:

$$\mathbf{B} \;=\; \mu_0\mu_r(\mathbf{H} + \mathbf{H}_0). \tag{7.5}$$

Here,

μ_0	denotes the permeability of the vacuum, $\mu_0 := 4\pi \cdot 10^{-7}\ \frac{Vs}{Am}$, and
μ_r	denotes the relative permeability.

In the case of permanent magnetic materials, $-\mathbf{H}_0$ is called the magnetic field where the induction $\mathbf{B}$ disappears. For the quantities which are not permanent magnetic we assume that $\mathbf{H}_0 = 0$.

We neglect the effects of hysteresis, such that the relative permeability μ_r can be represented as a function of $|\mathbf{B}|$, such that

$$\mathbf{B} \;=\; \mu_0\mu_r(|\mathbf{B}|)\cdot(\mathbf{H}+\mathbf{H}_0). \tag{7.6}$$

Additionally we introduce another quantity, the so-called *reluctivity*

$$\nu(|\mathbf{B}|) \;:=\; \frac{1}{\mu_0\mu_r(|\mathbf{B}|)}, \tag{7.7}$$

such that following relation holds:

$$\mathbf{H}+\mathbf{H}_0 \;=\; \nu(|\mathbf{B}|)\mathbf{B}. \tag{7.8}$$

Additionally the reluctivity ν may depend on the position x, i.e. $\nu(x,|\mathbf{B}|)$. Within one and the same material, ν is independent of the position. In the following discussion we only use the notation $\nu(|\mathbf{B}|)$. The dependency on the position x is only relevant from Chapter 8 on.

Since $\mathbf{B}$ is divergence free, we can find a vector potential $\mathbf{A}$ such that

$$\mathbf{B} \;=\; curl\ \mathbf{A}. \tag{7.9}$$

Considering the low-frequency case of electromagnetism, displacement currents are negligible in comparison with the impressed currents, i.e.,

$$\left|\frac{\partial \mathbf{D}}{\partial t}\right| \;\ll\; |\mathbf{J}|.$$

So we are left with the following reduced set of equations, the stationary (no dependence on t) magnetostatic formulation:

$$\begin{aligned} curl\ \mathbf{H} &= \mathbf{J}, \\ div\ \mathbf{B} &= 0, \\ \mathbf{H}+\mathbf{H}_0 &= \nu(|\mathbf{B}|)\mathbf{B}. \end{aligned}$$

By writing $\mathbf{H}$ and $\mathbf{B}$ in terms of the vector potential $\mathbf{A}$ we arrive at the magnetostatic vector potential formulation,

$$curl\ (\ \nu(|\ curl\ \mathbf{A}|)\cdot curl\ \mathbf{A}\ ) \;=\; \mathbf{J}+curl\ \mathbf{H}_0. \tag{7.10}$$

Before we perform further simplifications to the model we first inspect the reluctivity ν.

7.1.2 Material laws

The material influence appears in form of the reluctivity ν. We can differentiate between three different kinds of materials: linear materials, where the reluctivity ν is a constant, permanent magnetic materials and nonlinear materials.

Linear Materials:
The most famous linear material is vacuum. It is well known, that vacuum behaves linearly, i.e.,

$$\begin{aligned} \mu_r &\equiv 1, \\ \nu &\equiv \frac{1}{\mu_0} =: \nu_0, \end{aligned}$$

where we recall that $\mu_0 = 4\pi \cdot 10^{-7} \frac{Vs}{Am}$ denotes the permeability of vacuum. For electromagnetic problems we can assume that air behaves just like vacuum.

Permanent magnetic Materials:
For permanent magnetic materials we have the following material influence:

$$\mu_r \equiv 1.$$

From the previous section we know that for permanent magnetic materials we can assume

$$\mathbf{H}_0 \neq 0.$$

Thus, for permanent magnetic materials the relation (7.8) is given by

$$\mathbf{H} = \underbrace{\frac{1}{\mu_0}}_{=: \nu_0} \mathbf{B} - \mathbf{H}_0.$$

Nonlinear Materials:
In this thesis we neglect hysteresis effects. In this case there exists a bijective mapping $f : {\mathbb{R}_0}^+ \to {\mathbb{R}_0}^+$ such that

$$|\mathbf{B}| = f(|\mathbf{H}|). \tag{7.11}$$

The function f is called *B-H-curve* or *magnetization curve*. For large values of H the degree of amplification behaves again like in vacuum - in this case we say the material is saturated. These properties are summarized in the following assumption:

Assumption 7.1. *Any* B-H-curve

$$f : {\mathbb{R}_0}^+ \to {\mathbb{R}_0}^+$$

describing the relation $|\boldsymbol{B}| = f(|\boldsymbol{H}|)$ *fulfills the following conditions:*

1. f *is continuously differentiable,*
2. $f(0) = 0$*,*
3. $f'(s) \geq \mu_0$*,* $\forall s \geq 0$*,*
4. $f'(s) \overset{s\to\infty}{\longrightarrow} \mu_0$*.*

From (7.8), (7.11) and the assumption $\mathbf{H}_0 = 0$ for nonpermanent magnetic materials we know

$$\nu(|\mathbf{B}|) = \frac{|\mathbf{H}|}{|\mathbf{B}|} = \frac{f^{-1}(|\mathbf{B}|)}{|\mathbf{B}|}.$$

So the reluctivity ν is related to f via

$$\nu(s) \quad := \quad \frac{f^{-1}(s)}{s}. \tag{7.12}$$

7.2 Mathematical Model

7.2.1 Reduction to 2D

We consider a magnetic field problem on the x_1x_2- plane. It is requested, that the electric current density $\mathbf{J}$ is perpendicular to the magnetic field $\mathbf{H}$, which should lie on the x_1x_2- plane and that both fields are independent of x_3, i.e.

$$\mathbf{J} = \begin{pmatrix} 0 \\ 0 \\ J_3(x_1, x_2) \end{pmatrix}, \quad \mathbf{H} = \begin{pmatrix} H_1(x_1, x_2) \\ H_2(x_1, x_2) \\ 0 \end{pmatrix}. \tag{7.13}$$

Additionally, we assume that

$$\mathbf{H}_0 = \begin{pmatrix} H_{01}(x_1, x_2) \\ H_{02}(x_1, x_2) \\ 0 \end{pmatrix}.$$

From this assumption we obtain

$$curl\ \mathbf{H}_0 = \begin{pmatrix} 0 \\ 0 \\ -\frac{\partial}{\partial x_2} H_{01} + \frac{\partial}{\partial x_1} H_{02} \end{pmatrix}. \tag{7.14}$$

From the B-H-relation (7.6), we immediately get that $\mathbf{B}$ has the form

$$\mathbf{B} = \begin{pmatrix} B_1(x_1, x_2) \\ B_2(x_1, x_2) \\ 0 \end{pmatrix}.$$

Since the third component vanishes and $\mathbf{B} = curl\ \mathbf{A}$, we find that

$$(curl\ \mathbf{A})_3 = \frac{\partial A_2}{\partial x_1} - \frac{\partial A_1}{\partial x_2} = 0,$$

which leads to the following ansatz representing the vector potential

$$\mathbf{A} = \mathbf{A}(x_1, x_2) = \begin{pmatrix} 0 \\ 0 \\ A_3(x_1, x_2) \end{pmatrix}. \tag{7.15}$$

We conclude that

$$\mathbf{B} = curl\ \mathbf{A} = \begin{pmatrix} \frac{\partial A_3}{\partial x_2} \\ -\frac{\partial A_3}{\partial x_1} \\ 0 \end{pmatrix}. \tag{7.16}$$

Combining (7.10), (7.13), (7.14) and (7.15), we obtain

$$-div(\ \nu(\ |\nabla A_3|\ )\ \nabla A_3) \ \ = \ \ J_3 + (curl\ \mathbf{H}_0)_3. \tag{7.17}$$

From now on, the unknown A_3 will be identified by u:

$$u \ \ := \ \ A_3.$$

To summarize, our $2D$ reduction yields to the scalar partial differential equation

$$-div(\ \nu(\ |\nabla u|\ )\ \nabla u) \ \ = \ \ J_3 - \frac{\partial}{\partial x_2} H_{01} + \frac{\partial}{\partial x_1} H_{02}. \tag{7.18}$$

Additionally appropriate boundary conditions are needed. Let $\Omega \in \mathbb{R}^2$ be a

bounded domain with sufficiently smooth boundary $\Gamma = \partial\Omega$. Therefore, we require that the normal component of the magnetic induction $\mathbf{B}$ vanishes on the whole boundary Γ, i.e.

$$\mathbf{B} \cdot \vec{n} \;=\; 0 \quad \text{on } \Gamma,$$

where $\vec{n} = \vec{n}(x)$ denotes the outer unit normal vector to Γ at $x \in \Gamma$. This boundary condition can be written in terms of $\mathbf{A}$, i.e.

$$0 = \mathbf{B} \cdot \vec{n} \;=\; (curl\ \mathbf{A}) \cdot \vec{n} \quad \text{on } \Gamma.$$

It can be shown (cf. [11]), that it is possible to replace this boundary condition by

$$\vec{n} \times \mathbf{A} \;=\; 0.$$

This leads to

$$0 = \vec{n} \times \mathbf{A} = \begin{pmatrix} n_2 A_3 \\ -n_1 A_3 \\ 0 \end{pmatrix} \Longleftrightarrow A_3 = 0,$$

and, therefore

$$u \;=\; 0 \quad \text{on } \Gamma.$$

This is a homogeneous Dirichlet boundary condition. Finally the problem is completely reduced to 2D and by summarizing we have

$$-div(\ \nu(\ |\nabla u|\ )\ \nabla u) \;=\; J_3 - \frac{\partial}{\partial x_2} H_{01} + \frac{\partial}{\partial x_1} H_{02} \quad \text{in } \Omega, \tag{7.19}$$

$$u \;=\; 0 \quad \text{on } \Gamma. \tag{7.20}$$

7.2.2 Variational Formulation

From Figure 7.1 it is easy to see that the computational domain Ω consists of several different materials. Therefore we have to incorporate so-called interface conditions in the variational formulation. Therefore the physical interface conditions are of enormous importance. A comprehensive observation of this incorporation can be found in [12]. As a result it is easy to see that the interface conditions cancel out and thus, the variational formulation is the same as for a computational domain Ω consisting out of only one material.

For the variational formulation we consider the two Sobolev spaces

$$V = H^1(\Omega) \;\; = \;\; \{v \in L^2(\Omega) : \nabla v \in L^2(\Omega)\} \tag{7.21}$$

and

$$V_0 \;\; = \;\; \{v \in V : v = 0 \text{ on } \Gamma\}. \tag{7.22}$$

The variational formulation is obtained by multiplying both sides in (7.19) with an arbitrary test function $v \in V_0$ and integrating over the computational domain Ω. Integration by parts for the principal part and incorporating the boundary conditions (7.20) and the interface conditions leads to the following nonlinear variational formulation of the boundary value problem:

Find $u \in V_g$, such that

$$a(u, v) = \langle F, v\rangle \quad \forall v \in V_0, \tag{7.23}$$

where

$$\begin{aligned} a(u, v) \;\; &= \;\; \int_\Omega \nu(|\nabla u|)\nabla u \cdot \nabla v dx, \\ \langle F, v\rangle \;\; &= \;\; \int_\Omega \Big[J_3\; v \; + H_{01}\frac{\partial v}{\partial x_2} - H_{02}\frac{\partial v}{\partial x_1}\Big] dx, \end{aligned}$$

and

$$V_g \;\; = \;\; \{v \in V = H^1(\Omega) : v = 0 \text{ on } \Gamma\} = V_0.$$

On the right hand side of the variational formulation we also use integration by parts.

In (7.23) the expression $a(w, v)$ is only linear in the second argument v, but not necessarily in w. It is relatively easy to show that $a(u, \cdot)$ is bounded for each fixed $u \in V_0$ and that F is a bounded linear form, in short $F \in V_0^*$. Then our problem can be rewritten as an operator equation in the dual space

$$A(u) \;\; = \;\; F \quad in\; V_0^* \;\; , \tag{7.24}$$

with the nonlinear operator $A : V_0 \to V_0^*$ defined by the relation

$$\langle A(u), v\rangle \;\; = \;\; a(u, v), \tag{7.25}$$

so it follows

$$\langle A(u), v\rangle = \int_\Omega \nu(|\nabla u|)\nabla u \cdot \nabla v dx.$$

7.2.3 Existence and Uniqueness of the Solution

Existence and uniqueness of the solution to linear variational formulations is guaranteed by the Lax-Milgram theorem under suitable assumptions, in particular, ellipticity and boundedness of the bilinear form $a(\cdot,\cdot)$. In the nonlinear case, the operator equation (7.24) can be treated with a generalization of the Lax-Milgram theorem if the operator A is strongly monotone and Lipschitz continuous. These properties are investigated in detail in [12]. For existence and uniqueness we use Zarantonello's theorem, which is also known as the nonlinear Lax-Milgram theorem (cf. [14]).

Theorem 7.2. *(Zarantonello)*
Let $(V,(\cdot\,,\cdot\,)_V,\|\cdot\|_V)$ be a Hilbert space, $F\in V^*$ and $A:V\to V^*$ a nonlinear operator, fulfilling the following conditions:

1. *A is strongly monotone, i.e. $\exists c_1 = const > 0$:*

$$\langle A(u)-A(v),u-v\rangle \;\geq\; c_1\|u-v\|_V^2,\ \forall u,v\in V \tag{7.26}$$

2. *A is Lipschitz continuous, i.e. $\exists c_2 = const > 0$:*

$$\|A(u)-A(v)\|_{V^*} \;\leq\; c_2\|u-v\|_V,\ \forall u,v\in V \tag{7.27}$$

Then the operator equation

$$A(u)=F \quad in\ V^* \tag{7.28}$$

has a uniquely determined solution $u^*\in V$.

Proof. The proof is based on Banach's fixed point theorem (see [12]). □

Chapter 8

A 1D Model Problem and its Discretization

For simplicity we consider now a one dimensional problem. Section 8.1 starts with a short introduction to the theory of finite elements, which we afterwards apply to the variational setting of our PDE. At the end of this chapter (Section 8.3) we discuss the approximation of the B-H-curve (cf. [11],[1] and [12]). Most of the concepts given in this chapter can be generalized to two dimensions.

Starting point of the discussion is the following model problem:
Let $\Omega = (a, b)$ be a bounded domain with the boundary $\partial\Omega = \Gamma = \Gamma_D = \{a\} \cup \{b\}$. Find a function $u \in C^2(\Omega) \cap C(\Omega \cup \Gamma)$, such that the differential equation

$$-\Big[\nu\Big(|u'(x)|\Big)u'(x)\Big]' = J(x) + \frac{dH_0}{dx} \quad \forall x \in (a, b) \tag{MP 1}$$

and the homogenous Dirichlet boundary conditions

$$\begin{aligned} u(a) &= 0 \\ u(b) &= 0 \end{aligned}$$

are satisfied.

Applying the technique discussed in Chapter 7 the variational formulation reads (a complete derivation can be found in [12]):

Find $u \in V_g$, such that

$$a(u, v) = \langle F, v \rangle \quad \forall v \in V_0, \tag{8.1}$$

where

$$\begin{aligned} a(u,v) &= \int_a^b \nu(|u'(x)|)u'(x)v'(x)dx, \\ \langle F, v\rangle &= \int_a^b [J(x)v(x) - H_0(x)v'(x)]dx, \end{aligned}$$

and

$$\begin{aligned} V_0 &= \{v \in V = H^1(a,b) : v = 0 \text{ on } \Gamma\}, \\ V_g &= \{v \in V = H^1(a,b) : v(a) = 0 \wedge v(b) = 0\} = V_0. \end{aligned}$$

8.1 Finite Element Method for the Boundary Value Problem

We now give a short introduction to finite element method (cf. [12] and [14]). First of all we discretize the interval $[a,b]$ into N_h subintervals by introducing nodes $x_i, i = 0, \ldots, N_h$, with

$$a = x_0 < x_1 < \cdots < x_{N_h} = b.$$

We obtain a subdivision $\mathcal{T}_h$ as a set of subintervals $T_k = (x_{k-1}, x_k)$ for $k = 1, \ldots, N_h$. The mesh size h_k of each subinterval is given by

$$h_k = |x_{k-1} - x_k|.$$

Let P_k be the set of all polynomials of degree $\leq k$. V_h is the set of all continuous and piecewise affine linear functions on Ω, given by

$$V_h = \{v \in C(\bar{\Omega}) : v\Big|_T \in P_1 \ \ \forall T \in \mathcal{T}_h\}.$$

The nodal basis for V_h reads as follows. For each node $x_i, i = 0, \ldots, N_h$ we define the basis functions $\varphi_i \in V_h$ by

$$\varphi_i(x_j) = \delta_{ij} \qquad \forall i, j = 0, \ldots, N_h,$$

where δ_{ij} is the Kronecker symbol given by

$$\delta_{ij} = \begin{cases} 1 & \text{for } i = j, \\ 0 & \text{otherwise.} \end{cases}$$

One immediately sees that $\{\varphi_i : i = 0, \ldots, N_h\}$ is a basis of V_h, in particular each function $v_h \in V_h$ can be written in the form

$$v_h(x) = \sum_{i=0}^{N_h} v_i \varphi_i(x)$$

with $v_i = v_h(x_i)$.

• Test functions: $v_h\Big|_\Gamma = 0$:

$$V_{0h} = \{v_h \in V_h : v_h(a) = v_h(b) = 0\} = \{v_h \in V_h : v_h = \sum_{i=1}^{N_h-1} v_i \varphi_i\}$$

• Linear manifold for the solution: $v_h(a) = 0 \wedge v_h(b) = 0$:

$$V_{gh} = \{v_h \in V_h : v_h(a) = 0 \wedge v_h(b) = 0\} = \{v_h \in V_h : v_h = \sum_{i=1}^{N_h-1} v_i \varphi_i\}$$

One easily sees that $V_{0h} \subset V_0$ and $V_{gh} = V_{0h} \subset V_g$.

In the next step we use the following ansatz for the approximate solution:

$$u_h \quad = \quad \sum_{j=1}^{N_h-1} u_j \varphi_j,$$

i.e. $u_h \in V_{gh}$. We require that this approximate solution satisfies the variational formulation (9.5) for all test functions $v \in V_{0h}$, in other words

$$a(\sum_{j=1}^{N_h-1} u_j \varphi_j, \sum_{i=1}^{N_h-1} v_i \varphi_i) \quad = \quad \langle F, \sum_{i=1}^{N_h-1} v_i \varphi_i \rangle$$

for all $v_i \in \mathbb{R}, i = 1, \ldots, N_h - 1$.

Because of the linearity of $a(\cdot, \cdot)$ in the second argument, it suffices to test only with the basis functions φ_i.

$$a(\sum_{j=1}^{N_h-1} u_j \varphi_j, \varphi_i) \quad = \quad \langle F, \varphi_i \rangle$$

for all $i = 1, \ldots, N_h - 1$.

Summarizing, we get a nonlinear system of equations:

Find $\underline{u}_h = [u_j]_{j=\overline{1,N_h-1}}$ such that the nonlinear system of equations

$$\underline{K}_h[\underline{u}_h] \;=\; \underline{f}_h \tag{8.2}$$

is fulfilled in $\mathbb{R}^{N_h-1}$ with the nonlinear map $\underline{K}_h : \mathbb{R}^{N_h-1} \to \mathbb{R}^{N_h-1}$ given by

$$\underline{K}_h[\underline{w}_h] = [\underline{K}_h[\underline{w}_h]]_i = [a(\sum_{j=1}^{N_h-1} w_j\varphi_j, \varphi_i)]_i$$

for all $i = 1, \ldots, N_h - 1$ and

$$\underline{f}_h = [f_h]_i = \langle F, \varphi_i\rangle.$$

For any arbitrary u we define

$$a[u](w, v) \;:=\; \int_a^b \nu(|u'(x)|)w'(x)v'(x)dx,$$

then, of course

$$a(u, v) \;=\; a[u](u, v).$$

Obviously we have the relation

$$a[u_h](w_h, v_h) \;=\; (K_h[\underline{u}_h]\underline{w}_h, \underline{v}_h).$$

Therefore

$$\underline{K}_h[\underline{u}_h] \;=\; K_h[\underline{u}_h]\underline{u}_h,$$

where $K_h[\underline{u}_h]$ is a $(N_h - 1) \times (N_h - 1)-$ matrix, which can be generated element-wise like the stiffness matrix in the linear case.

The element stiffness matrices reads

$$K_h^{(k)} = \begin{pmatrix} \int_{T_k} \nu(|u_h'|)\varphi_{k-1}'(x)^2dx & \int_{T_k} \nu(|u_h'|)\varphi_{k-1}'(x)\varphi_k'(x)dx \\ \\ \int_{T_k} \nu(|u_h'|)\varphi_k'(x)\varphi_{k-1}'(x)dx & \int_{T_k} \nu(|u_h'|)\varphi_k'(x)^2dx \end{pmatrix}.$$

Since u_h' is constant on T_k, $\nu(|u_h'|)$ is also constant on T_k. So we are able to

put the term $\nu(|u_h'|)$ considered on the elements T_k in front of the integrals, such that the following identity holds:

$$\int_{T_k} \nu\Big(|u_h'|\Big)\psi(x)dx \;=\; \nu\Big(|u_h'\Big|_{T_k}|\Big)\int_{T_k}\psi(x)dx.$$

By mapping each element T_k to the reference element $\hat{T} = (0,1)$ and assembling the stiffness matrix element-wise it is easy to show that the stiffness matrix K_h is a tridiagonal matrix (cf. [12]).

The same technique is used to compute the load vector. For the not exactly computable integrals in the element load vector

$$f_h^{(k)} \;=\; \begin{pmatrix} \int_{T_k}\Big[f(x)\varphi_{k-1}(x) - H_0(x)\varphi_{k-1}'(x)\Big]dx \\ \\ \int_{T_k}\Big[f(x)\varphi_k(x) - H_0(x)\varphi_k'(x)\Big]dx \end{pmatrix}.$$

we use a so-called quadrature rule. In the implementation of our program we use the trapezoidal rule

$$\int_a^b g(x)dx \;\approx\; \frac{b-a}{2}[g(a)+g(b)].$$

To apply Newton's method it is also required to compute the Jacobian matrix. Therefore we have to compute the (Gâteaux-)derivative of $a[u]$. It turns out that the Jacobian is also a tridiagonal matrix. For more details of this computation techniques we refer to [12].

8.2 The geometry of the motor

Let us consider the one-dimensional model of our motor in Figure 8.1. We

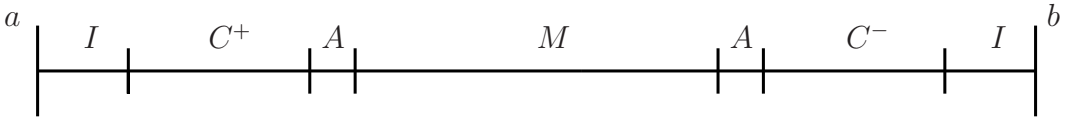

Figure 8.1: One-dimensional model of a motor

have the following regions:

I	iron
C^+	coil
A	air
M	permanent magnet
C^-	coil

For these regions we have the following assumptions:

$$\nu(x,\cdot) := \begin{cases} \nu_{iron}(\cdot), & \text{for } x \in \Omega_{iron} \quad \text{(iron)} \\ \nu_0 = \text{const}, & \text{elsewhere} \quad \text{(coil,air,magnet)} \end{cases}$$

$$J(x) := \begin{cases} J_3 = \text{const}, & \text{for } x \in \Omega_{C^+} \quad \text{(coil)} \\ -J_3, & \text{for } x \in \Omega_{C^-} \quad \text{(coil)} \\ 0 & \text{elsewhere} \quad \text{(iron,air,magnet)} \end{cases}$$

$$H_0(x) := \begin{cases} H_{01} = \text{const}, & \text{for } x \in \Omega_M \quad \text{(magnet)} \\ 0 & \text{elsewhere} \quad \text{(iron,coil,air)} \end{cases}$$

For $\nu_{iron}(\cdot)$ we use the analytic function described in Section 8.3.

8.3 B-H-Curve Approximation

From Subsection 7.1.2 we know, that B-H-curves (or magnetization curves) are needed for the modeling of ferromagnetic materials in connection with electromagnetic field computation. Due to the underlying physics, such curves are naturally monotone and must often be approximated from real-life measurements (see Figure 8.2). In practice such material curves are never given analytically. A technique for an approximation of such a B-H-curve based on the use of spline functions and a data depending smoothing functional is treated by [11, 1].

In this work we consider an analytic function, which should approximate the inverse $f^{-1}(s)$ of the real B-H-curve and fulfills Assumption 7.1. In our program the following analytic function (see Figure 8.3) is used:

$$f^{-1}(s) := \begin{cases} \alpha s + e^{\beta s} + \gamma & \text{for } s < s_0, \\ \eta s + \theta & \text{otherwise,} \end{cases}$$

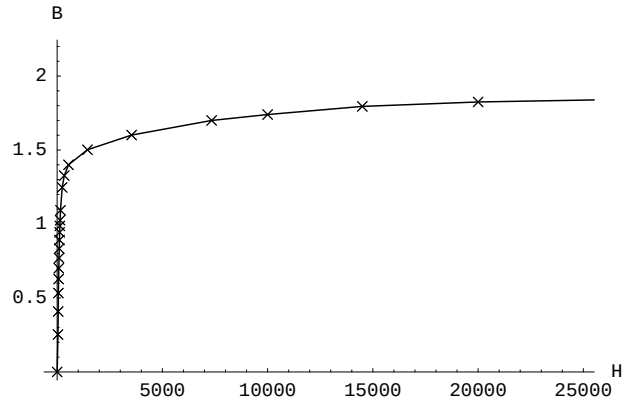

Figure 8.2: B-H-Curve from real-life measurements

where $\alpha, \beta, \gamma, \eta, \theta \in \mathbb{R}$.

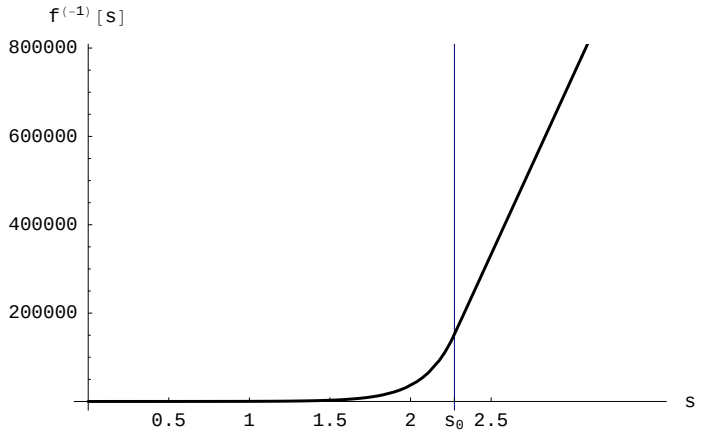

Figure 8.3: $f^{-1}(s)$

These coefficients are chosen such that $f^{-1}(s)$ is a good approximation of the magnetization curve. The nonlinearity occurs in this material relation between the magnetic field $\mathbf{H}$ and the magnetic induction $\mathbf{B}$. This nonlinear relation can be described by the reluctivity ν, which is given via (7.12) by

$$\nu(s) \quad := \quad \frac{f^{-1}(s)}{s}.$$

Chapter 9

A Parameter Dependent Problem

In this chapter we want simulate the behavior of the electric motor which we discussed in Chapter 7. This is a parameter dependent problem as we discussed it in Chapter 6. We apply a numerical path following method to follow the solution curve.

Recall our model problem of the motor in Figure 7.1. The group in the ACCM (Austrian Center of Competence in Mechatronics) uses a program called FEMAG for the analysis and simulation of such electric machines. One of their applications is the shape optimization of electric motors by simulation, where the rotor is rotated in steps of 2° in the interval of 60°.

Our main task now is to simulate the behavior of the electric motor. The natural parameter involved in this problem is an angle φ, such that

$$H(u, \varphi) \;=\; 0. \tag{9.1}$$

Starting point of our consideration is the electric motor at rest. In other words we consider a relative position between the rotor and the stator of the motor. An example of such a start position can be seen in the left picture of Figure 9.1.

The first step now is to turn the rotor in one direction by an angle φ_1 (see Figure 9.1(right)) and consider this position. We know that the rotor is a permanent magnet. The current density $\mathbf{J}$ takes different values in different coils. Hence, it is easy to see that the problem changes by turning the rotor by the angle φ_1. If we repeat this step again and again (cf. Figure 9.2) we obtain a sequence of different problems for all angles φ. So, of course this is a

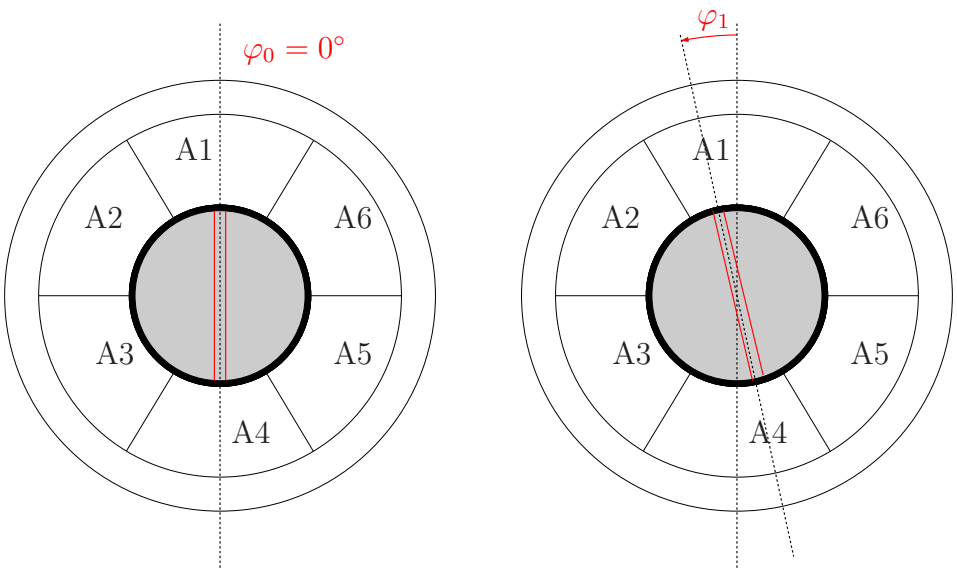

Figure 9.1: Rotation of the motor: Starting position and first rotation step

parameter dependent problem. Now we are able to describe the behavior of the solution with respect to the parameter φ. A consequence of this is that now we obtained some information about the behavior of the magnetic field $\mathbf{H}$ during a rotation process.

For simplicity we consider a one-dimensional cut of the electric motor (see Figure 9.3). We now try to derive an analogon to the rotation steps discussed above in the two-dimensional problem. From the previous discussion we know that for every parameter φ we have a different problem. In our one-dimensional model problem we change in every step the length of the coils C^+ and C^-. This describes approximately the two-dimensional simulation.

For simplicity we neglect the magnetization term H_0, such that the problem reads as follows:

Let $\Omega = (a, b)$ be a bounded domain with the boundary $\partial\Omega = \Gamma = \Gamma_D = \{a\} \cup \{b\}$. Find a function $u \in C^2(\Omega) \cap C(\Omega \cup \Gamma)$, such that the differential equation

$$-\Big[\nu\Big(|u'(x)|\Big)u'(x)\Big]' = J(x) \quad \forall x \in (a, b) \tag{MP 2}$$

and the homogenous Dirichlet boundary conditions

$$\begin{aligned} u(a) &= 0 \\ u(b) &= 0 \end{aligned}$$

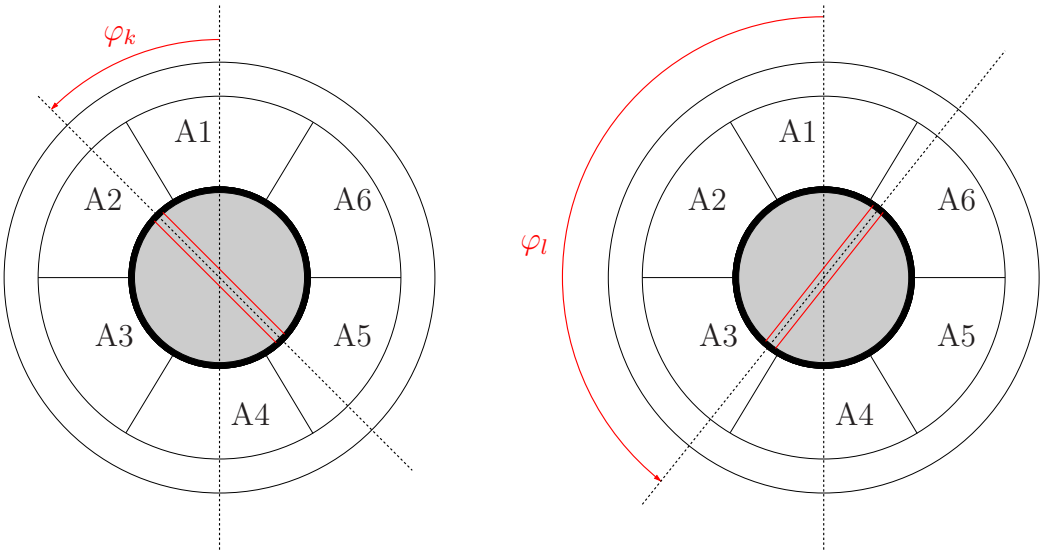

Figure 9.2: Rotation of the motor: k-th and l-th rotation step

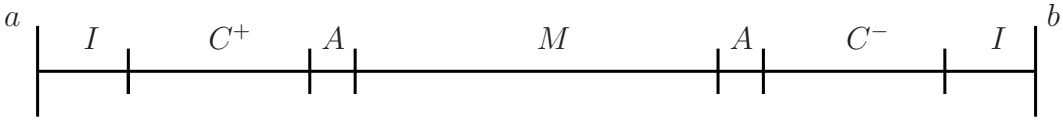

Figure 9.3: One-dimensional model of a motor with fixed interfaces

are satisfied.

We again consider assumptions on the areas

$$\nu(x,\cdot) := \begin{cases} \nu_{iron}(\cdot), & \text{for } x \in \Omega_{iron} \quad \text{(iron)} \\ \nu_0 = \text{const}, & \text{elsewhere} \quad \text{(coil,air,magnet)} \end{cases} \tag{9.2}$$

$$J(x) := \begin{cases} J_3 = \text{const}, & \text{for } x \in \Omega_{C^+} \quad \text{(coil)} \\ -J_3, & \text{for } x \in \Omega_{C^-} \quad \text{(coil)} \\ 0 & \text{elsewhere} \quad \text{(iron,air,magnet)} \end{cases} \tag{9.3}$$

So far we only considered fix interfaces like in Figure 9.3. In order to simulate the behavior of the motor we move the interfaces from Figure 9.3. This can be done in the following way:

Starting point is the geometry in Figure 9.4. It is easy to see that the coil C^+ is located on the interval $[c_l, c_l^{start}]$ and the coil C^- is located on the interval $[c_r, c_r^{start}]$. Moreover the intervals $[c_l, c_l^{start}]$ and $[c_r, c_r^{start}]$ both have length l_C.

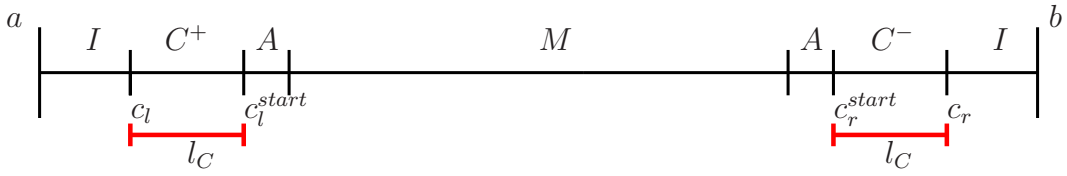

Figure 9.4: Start-configuration

Now we try to move the interfaces c_l^{start} and c_r^{start} in that direction such that the length l_C is either enlarged or reduced to a new length l_C^{end}. In the following discussion we only consider the case where we enlarge the length of the intervals. So we obtain a new geometry, which can be seen in Figure 9.5.

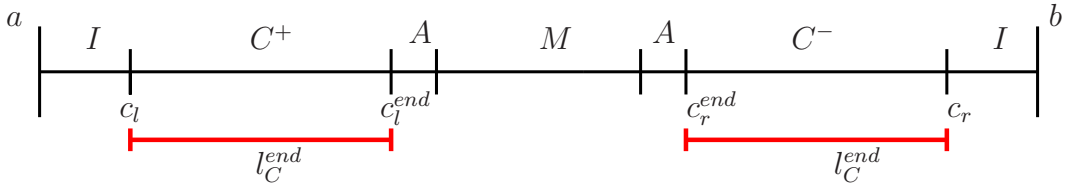

Figure 9.5: End-configuration

We obtain the end-configuration step-wise from the start-configuration in the following way: We fix the interface c_l. Then the new interface $c(t)$ is obtained by choosing a parameter $t \in [0, 1]$ such that

$$c(t) \quad = \quad (1-t)c_l^{start} + tc_l^{end}, \tag{9.4}$$

where c is the actual position of the interface and $c \in [c_l^{start}, c_l^{end}]$. So for $t = 0$ we obtain c_l^{start} and for $t = 1$ we obtain c_l^{end}. This holds for the area of the coil C^+. A similar way is used for the coil C^-.

Applying the technique discussed in Chapter 7 the variational formulation for this differential equation reads:

Find $u \in V_g$, such that

$$a(u,v) = \langle F, v \rangle \quad \forall v \in V_0, \tag{9.5}$$

where

$$\begin{aligned} a(u,v) &= \int_a^b \nu(|u'(x)|)u'(x)v'(x)dx, & (9.6)\\ \langle F, v \rangle &= \int_a^b [J(x)v(x)]dx, & (9.7) \end{aligned}$$

and

$$\begin{aligned} V_0 &= \{v \in V = H^1(a,b) : v = 0 \text{ on } \Gamma\},\\ V_g &= \{v \in V = H^1(a,b) : v(a) = 0 \wedge v(b) = 0\} = V_0. \end{aligned}$$

The stiffness matrix K_h and the load vector $\underline{f}_h$ can be generated like we discussed in Chapter 8. From the assumptions (9.2), (9.3) and equation (9.4) it immediately follows that the electric current density J depends on the parameter t and the space x. Therefore the load vector depends also on t, but not the stiffness matrix K_h. Thus we obtain the nonlinear system of equations

$$K_h \underline{u}_h = \underline{f}_h(t).$$

The right hand side (9.7) can be divided in the following way:

$$\begin{aligned} \int_a^b J(x)v(x)dx &= \int_a^{c_l} J(x)v(x)dx + \int_{c_l}^{c(t)} J(x)v(x)dx + \int_{c(t)}^{b-c(t)} J(x)v(x)dx + \\ &+ \int_{b-c(t)}^{c_r} J(x)v(x)dx + \int_{c_r}^{b} J(x)v(x)dx. \end{aligned}$$

From (9.3) we know that J vanishes on the areas iron, air and magnet. Thus we obtain

$$\int_a^b J(x)v(x)dx = \int_{c_l}^{c(t)} J(x)v(x)dx + \int_{b-c(t)}^{c_r} J(x)v(x)dx. \tag{9.8}$$

Now we only consider the coil C^+ (similar for C^-), i.e. the integral

$$\int_{c_l}^{c(t)} J(x)v(x)dx. \tag{9.9}$$

In the interval $[c_l, c(t)]$ the electric current density J is constant.
By taking basis function φ_i as we discussed it in Chapter 8 the integral from (9.9) reads

$$J_3 \int_{c_l}^{c(t)} \varphi_i(x)dx \quad := \quad f_i(t).$$

Now we are able to set up a path-following procedure. We start again at a known initial point

$$u^0 \quad = \quad (x^0, t^0) \in \mathbb{R}^{n+1}$$

such that

$$H(u^0) \quad = \quad 0, \tag{9.10}$$

where

$$H(u) = H(x,t) \quad = \quad F(x, c(t)) = K_h x - \underline{f}_h(t).$$

In the discussion from Chapter 4 we need the derivative of H with respect to x and t in order to set up an efficient method. The derivative with respect to x is the same as discussed in Chapter 4. For

$$\frac{\partial}{\partial t} H(x,t) \quad = \quad -\frac{\partial}{\partial t} f_h(t)$$

we use the following corollary (cf. [4]).

Corollary 9.1. *Let $f : [a,b] \to \mathbb{R}$ be continuous, $\varphi, \psi : [c,d] \to [a,b]$ be continuously differentiable and $g : [c,d] \to \mathbb{R}$ be given by*

$$g(t) := \int_{\varphi(t)}^{\psi(t)} f(x)dx.$$

Then g is differentiable and

$$g'(t) \quad = \quad f(\psi(t))\psi'(t) - f(\varphi(t))\varphi'(t)$$

holds for all $t \in [c,d]$.

Proof. The proof can be found in [4].

□

Using the results from Corollary 9.1 the derivative of the integral in (9.9) is given by

$$f_i'(t) \quad = \quad J_3 \varphi_i(c(t)) c'(t).$$

Finally we have

$$\frac{\partial}{\partial t} H(x,t) \quad = \quad -(f_i'(t))_{i=1,\ldots,N_h-1}.$$

Now everything what we need for a predictor-corrector method, as discussed in Chapter 4, is given.

Chapter 10

Numerical Results

This chapter consists of two major parts. On the one hand the discussed homotopy methods are tested on the one-dimensional model problem of an electric motor. In the second part some numerical results obtained by the numerical path following method for the parameter dependent problem are presented.

10.1 Homotopy Methods

In this section we present the numerical results obtained by a homotopy method applied to the one-dimensional model problem (MP 1) for fixed current density, magnetic field and the number of unknowns. For our problem, we set the following fixed values:

- $J_3 = 10^6$,
- $H_1 = 10^4$,
- $N_h = 10^4$.

For the initial vector for the method we use

$$u^0 = (0, 0, \ldots, 0)^T.$$

In this section we introduce the following notation:

- **Homotopy I**: A predictor-corrector method as discussed in Section 4.3, i.e. a predictor-corrector method with vertical corrector.
- **Homotopy II**: A predictor-corrector method as discussed in Section 4.4,

i.e. a predictor-corrector method with pseudo-arc length approximation.

The variable *iter* will measure how many times the Jacobian matrix has to be generated as well as how often the system of equations has to be solved, e.g. if $iter = 5$ we have to generate the Jacobian matrix and solve a system of equations 5 times.

We present the numerical results obtained by the two methods Homotopy I and Homotopy II with a fixed step length. In order to save computational cost we perform in each PC-step only one corrector step. So we don't go back to the solution curve in each PC-step. The last point obtained with these methods is used as a starting point for Newton's method in order to compute the exact solution.

There we use a stopping criterion

$$\|r_{new}\|_2 \leq \varepsilon \max\Big\{\|r_0\|_2, \|b\|_2\Big\}, \tag{10.1}$$

where

- r_{new} is the residual of the actual step,
- r_0 is the starting residual,
- b is the right hand side of equation (8.2), i.e. $b = \underline{f}_h$,
- $\varepsilon = 10^{-7}$

and for a vector $x \in \mathbb{R}^n$ we define the Euclidean norm

$$\|x\|_2 \;:=\; \Big(\sum_{i=1}^{n} |x_i|^2\Big)^{\frac{1}{2}}.$$

In Table 10.1 we see how many iterations we need for one fixed step length with the methods Homotopy I and Homotopy II, respectively.
These numerical results demonstrate the functionality of the implemented methods. It is easy to see the greater the step length is, the fewer iterations are needed in both methods. It is also easy to see for a step size 1.0 for the method Homotopy I we only need 2 iterations, i.e. we can easily solve this problem with classical Newton's method. The reason for this is that the order of nonlinearity is not high enough in our simplified problem.

step size	iter
1/10	20
1/5	10
1/2	4
1.0	2

step size	iter
100	22
500	6
1000	4
2000	3
3000	2

Table 10.1: Number of iterations for Homotopy I (left) and Homotopy II (right)

10.2 Numerical Results for a Parameter Dependent Problem

In this section we present some numerical results obtained by a numerical path following method applied to the problem (MP 2), which was discussed in Chapter 9. In this case it is important to go back to the curve after every predictor-corrector step. Therefore we use Newton's method as corrector method with the stopping criterion (10.1). For numerical experiments, we use an electric current density

$$J(x) := \begin{cases} 10^6, & \text{for } x \in \Omega_{C^+} \quad \text{(coil)} \\ -10^6, & \text{for } x \in \Omega_{C^-} \quad \text{(coil)} \\ 0 & \text{elsewhere} \quad \text{(iron,air,magnet)} \end{cases}$$

Moreover we set the number of unknowns $N_h = 10000$. Without loss of generality we can assume that the parameter $t \in [0, 1]$. In our consideration we want to have the same computational grid in every simulation step. For the two-dimensional problem we know that the rotor is turned by 2° steps. In the one-dimensional case the interval $[0, 1]$ is divided into $\xi = 500$ equidistant subintervals. So we guarantee that the computational grid for the whole domain is approximately uniform. Thus we have a step length of 1/500 and we need 500 predictor-corrector steps. In Figure 10.1 we see the nonlinear relation between the solution $\|u\|$ and the parameter t.

This result is obtained without a step length control. For such a problem we can also use a step size control which is a little bit different from the step length adaptation which was discussed in Chapter 5. In order to avoid get-

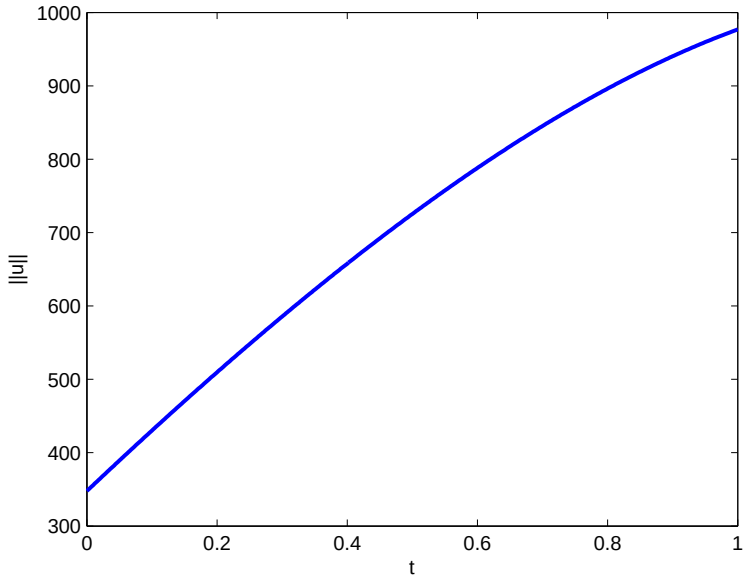

Figure 10.1: Numerical results of a predictor-corrector method without step length control

ting into troubles with the computational grid we only accept points which are multiples of $1/\xi$.

In order to have a reasonable magnitude of the two quantities $\widetilde{\kappa}$ and $\widetilde{\delta}$ we use relative values instead of absolute values. This can be handled in the following way:
We know the following relation for all $x \in \mathbb{R}^n$:

$$\|x\|_2 \leq \sqrt{n}\|x\|_\infty.$$

We use this estimate to scale the quantities for our step size controlling procedure. If we use the following notation

$$d_{ref} \quad := \quad \sqrt{N_h} u_{ref},$$

where u_{ref} denotes a reference value in the magnitude of the maximum norm of the solution of our problem, then we are able to scale the quantity $\widetilde{\delta}$ in the following sense:

$$\widetilde{\delta} \quad = \quad \widetilde{\delta}_{rel} d_{ref}$$

Now the quantity $\widetilde{\delta}$ can be chosen in the way described above.

In the following we present some numerical results obtained by applying a numerical path following method to a parameter dependent problem. Thereby we consider three different start step sizes σ and vary the quantities $\widetilde{\kappa}$ and $\widetilde{\delta}_{rel}$ for every start step size. In Table 10.2, Table 10.3 and Table 10.4 we see the so obtained results.

		$\widetilde{\delta}_{rel}$					
		0.6	0.75	1.0	1.5	3.0	5.0
$\widetilde{\kappa}$	1.1	18	20	21	22	21	21
	1.3	19	20	20	21	21	21
	1.5	21	22	22	22	22	22
	2.0	21	23	17	17	17	17
	5.0	21	23	16	18	16	16

Table 10.2: Number of iterations with start-step size $\sigma = 1/5$

		$\widetilde{\delta}_{rel}$					
		0.6	0.75	1.0	1.5	3.0	5.0
$\widetilde{\kappa}$	1.1	20	23	19	19	19	19
	1.3	20	24	20	20	20	20
	1.5	20	19	20	20	20	20
	2.0	20	20	20	20	20	20
	5.0	20	20	21	15	16	15

Table 10.3: Number of iterations with start-step size $\sigma = 1/8$

Summarized one can see that it is not easy to find an appropriate choice of $\widetilde{\kappa}$ and $\widetilde{\delta}_{rel}$ as we discussed it in Chapter 5. On the one hand if $\widetilde{\delta}_{rel}$ is large, we go very fast forward, but we need many corrector steps to come back to the solution curve. On the other hand if $\widetilde{\delta}_{rel}$ is small we traverse the curve very close. As a consequence of this choice the adapted step size is very small in order not to run out of the tube and therefore also many iterations are required.
If $\widetilde{\kappa}$ is small we have very accurate intermediate results, but therefore also many corrector steps are required.

		$\widetilde{\delta}_{rel}$					
		0.6	0.75	1.0	1.5	3.0	5.0
$\widetilde{\kappa}$	1.1	20	21	22	23	23	23
	1.3	20	23	25	19	19	19
	1.5	20	24	19	19	19	19
	2.0	20	25	20	20	20	20
	5.0	20	25	20	19	16	16

Table 10.4: Number of iterations with start-step size $\sigma = 1/10$

Also the starting step size σ plays a role in our consideration. One can see that for small σ we need more steps to go forward than for a greater starting step size σ. This is one consequence of the deceleration factor $f \in [\frac{1}{10}, 2]$.

Remark 10.1. In the beginning of this discussion we talked about improving the damped Newton's method. During this thesis it turns out that it is sufficient to solve our problem with classical Newton's method. The damped Newton method in this sense is too discreet. The reason for this disadvantage is that the order of nonlinearity is not high enough in our simplified problem, such that a desired improvement is achieved.

Chapter 11

Conclusion and Future Work

In this thesis, the homotopy methods for solving magnetostatic problems are thoroughly discussed. We introduce 2 different methods to compute the exact solution along a so-called solution curve. In order to obtain a better performance of such a method we discuss a step length adaptation procedure.

From the governing physical equations (Maxwell) we have reduced and derived an abstract mathematical formulation. Solvability has been proven under assumptions on the nonlinear parameter ν.

We have discretized the continuous problem with the Finite Element Method.

Numerical results have shown the efficiency of such methods applied to a one-dimensional electric motor model problem.

This work can be continued in the following directions:

1. Homotopy method for the 2D problem:
   So far we only considered homotopy methods for a one-dimensional problem. The discussed homotopy methods can be carried over in a similar sense.

2. Nonlinearity of the problem:
   In Chapter 10 we saw that the order of nonlinearity is harmless in order to see a strong improvement to classical Newton's method. If the reluctivity ν exhibits a high nonlinearity it is required to use homotopy methods to solve such problems.

Bibliography

[1] B. Jüttler & C. Pechstein. Monotonicity-preserving Interproximation of B-H-curves. *Journal of Computational and Applied Mathematics*, 196(1):45–57, 2006.

[2] H. D. Mittelmann & D. Roose. *Continuation Techniques and Bifurcation Problems*. Birkhäuser, 1989.

[3] B. C. Eaves, F. J. Gould, H. O. Peitigen, and M. J. Todd. *Homotopy Methods and Global Convergence*. Plenum Press, New York and London, 1983.

[4] H. W. Engl. *Skriptum Analysis*. Institut für Industriemathematik, Johannes Kepler Universität Linz, 2005.

[5] E. Frank. *Free-form Optimization of Electric Machines based on Shape Derivatives*. Johannes Kepler University Linz, 2010. Master Thesis.

[6] B. Heise. *Mehrgitter-Newton-Verfahren zur Berechnung nichtlinearer magnetischer Felder*. Technische Universität Chemnitz, 1991.

[7] M. Hermann. *Numerische Mathematik*. Oldenbourg, 2006.

[8] E. L. Allgower & K. Georg. *Numerical Continuation Methods*. Springer-Verlag, Heidelberg, 1990.

[9] M. Kollmann. *Shape Optimization with Shape Derivatives*. Johannes Kepler University Linz, 2008. Bachelor Thesis.

[10] U. Langer & M. Jung. *Methode der finiten Elemente für Ingenieure*. Teubner-Verlag, Stuttgart, Leipzig, Wiesbaden, 2001.

[11] C. Pechstein. *Multigrid-Newton-Methods for Nonlinear Magnetostatic Problems*. Johannes Kepler University Linz, 2004. Master Thesis.

[12] A. Lechner & S. Mühlböck. *Numerical solution of nonlinear stationary magnetic field problems*. Johannes Kepler University Linz, 2008. Bachelor Thesis.

[13] W. Zulehner. *Lecture Notes for the Course Numerical Analysis.* Johannes Kepler Universität Linz, Winter Semester 2005/06.

[14] W. Zulehner. *Lecture Notes for the Course Numerical Methods for Partial Differential Equations.* Johannes Kepler Universität Linz, Winter Semester 2005/06.

[15] W. Zulehner. *Lecture Notes for the Course Special numerical methods: Nonlinear equations.* Johannes Kepler Universität Linz, Winter Semester 2008/09.

[16] W. Zulehner. *Lecture Notes for the Course Numerical Methods for time-dependent Problems.* Johannes Kepler Universität Linz, Winter Semester 2009/10.

Index

B-H - Curve, 36
    Approximation, 47
    Assumptions, 36

Arclength, 14
Asymptotic Expansion, 24

Conclusion, 62
Continuation
    Method, 11
Contraction Rate, 25, 27
Curve Of Solutions, 13

Davidenko Differential Equation, 18
Dirichlet Boundary Condition
    Homogenuous, 39
Discretization, 42
Distance to Curve, 25, 29

Electric Current Density, 37
Electric Motor, 33
Embedding, 9
    Method, 11
Euler's Method, 18

FEM, 43
Finite Element Method, 43

Homotopy
    Convex Homotopy, 10
    Equation, 7, 9
    Global Homotopy, 9, 10
    Map, 9
    Method, 6, 11
    Parameter, 9
    Properties, 9

Implicitly Defined Curves, 12
Initial Value Problem, 6

Jacobian
    Matrix, 6

Lipschitz Continuous, 41
Load Vector, 46

Magnetic
    Field, 34
    Flux, 34
Magnetization Curve, 36
Magnetostatic Formulation, 35
Magnetostatic Problem, 33
Material Laws, 36
    Linear Materials, 36
    Nonlinear Materials, 36
    Permanent Magnetic Materials, 36
Mathematical Model, 37
Maxwell's Equations, 33
Model Problem
    One Dimensional, 42
      Variational Formulation, 42

Newton Path, 6
Newton's Method, 6
Numerical Path Following, 16, 31, 49
Numerical Results, 56
    Homotopy Methods, 56
    Parameter Dependent Problem, 58

Operator Equation, 40

Parameter Dependent Problem, 31, 49
Partial Differential Equation, 38
PC - Method, 19

Peremability
    Realtive, 34
Permeability
    Vacuum, 34
Physical Problem, 33
Predictor - Corrector Method, 19
Predictor Step, 21
Pseudo - Arc Length Approximation, 20

Regular Point, 13
Regular Value, 13
Reluctivity, 35

Solution
    Existence, 41
    Uniqueness, 41
Solution Curve, 13
Staircase Method, 16
Step Length
    Adaptation, 24
    Control, 24
Step Size
    Adaptation, 24
    Control, 24
Stiffness Matrix, 45
Strongly Monotone, 41

Tangent Vector, 20
Theorem
    Lax-Milgram, 41
    Zarantonello, 41
Tridiagonal Matrix, 46
Tube Along a Curve, 29
Turning Points, 14

Variational Formulation, 39
Vector Potential, 35
    Formulation, 35

Eidesstattliche Erklärung

Ich, Stefan Mühlböck, erkläre an Eides statt, dass ich die vorliegende Diplomarbeit selbständig und ohne fremde Hilfe verfasst, andere als die angegebenen Quellen und Hilfsmittel nicht benutzt bzw. die wörtlich oder sinngemäß entnommenen Stellen als solche kenntlich gemacht habe.

Zwettl an der Rodl, Mai 2010

_____

Stefan Mühlböck

Curriculum Vitae

Name: Stefan Mühlböck

Nationality: Austria

Date of Birth: 25 February, 1985

Place of Birth: Linz, Austria

Education:

1991-1995	Volksschule (elementary school), Zwettl an der Rodl
1995-1999	Hauptschule (secondary modern school), Bad Leonfelden
1999-2004	HTL for Electrotechnics, Linz
2005-2009	Baccalaureate studies in Technical Mathematics, Johannes Kepler University Linz
2009-2010	Master studies in Industrial Mathematics, Johannes Kepler University Linz

Special Activities: 23^{rd} ECMI Modeling Week, Wroclaw, Poland